Title
Comparative analysis of gene expression in developing chicken and mouse telencephalon

Author
Kuwana, Ellen Yoshino

Publication Date
1996

Peer reviewed|Thesis/dissertation

Comparative Analysis of Gene Expression in
Developing Chicken and Mouse Telencephalon

by

Ellen Yoshino Kuwana

THESIS

Submitted in partial satisfaction of the requirements for the degree of

MASTER OF SCIENCE

in

Biochemistry

in the

GRADUATE DIVISION

of the

UNIVERSITY OF CALIFORNIA

San Francisco

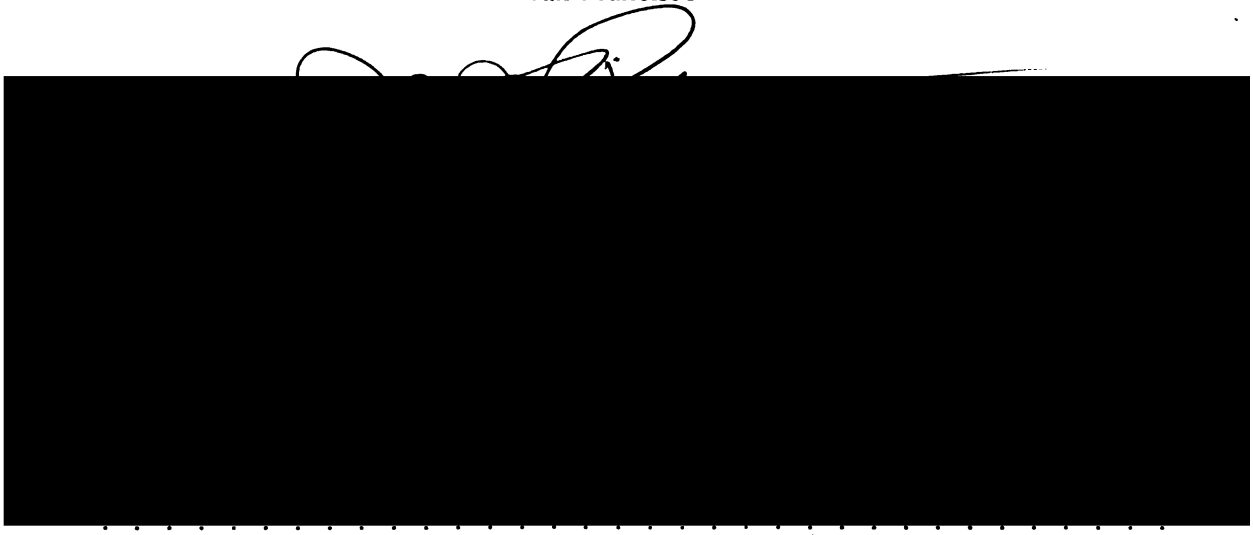

Date University Librarian

Degree Conferred: . . . . . .

to the chemists in my life

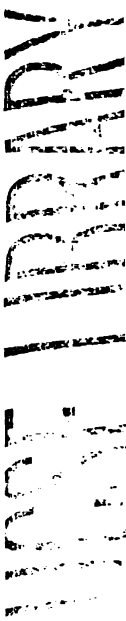

Preface

The cliché that the grass is greener on the other side certainly holds true for my experience at UCSF. When I was a research associate, I envied the freedom with which graduate students could come and go in the lab, the long coffee breaks, and the sense of camaraderie. Then I became a graduate student, and I realized how good I had it as a technician: an eight- or nine-hour workday, a salary, none of the politics or pressure of getting a project to work. In the end, I appreciate aspects of both paths, and plan to continue to be involved in science at some level, although probably more in the peripheral realm of science writing and/or science education.

As I think about who I want to, indeed must, thank, I am truly in awe of what wonderful friends I have at UCSF. And not only are they incredibly smart, but also supportive and generous with their time and expertise. The 14th floor, the Tessier-Lavigne, Bargmann, and Martin labs, was a wonderful home away from home. In particular, Kayvan Roayaie, Erin Peckol, Roberta Weber, Tito Serafini, Chen-Ming Fan, Dave Leonardo, and José de la Torre have always been supportive friends and people from whom I sought and received excellent advice. Marc Tessier-Lavigne and the rest of the lab really taught me how to do science, and how to do it well and efficiently. Marc is a role model for how to do everything well: science, writing, and choosing excellent tapas restaurants.

During the transition to graduate school, I was grateful for my prior experience in science, which gave me the confidence to pursue my goals, no matter how difficult or unlikely. I also am grateful to Charles Craik, John Watson, and Sue Adams for endless help and encouragement in navigating the program. After convincing Allison Doupe that she wanted someone in

her lab doing molecular biology, I tried designing and performing *in situ* hybridization techniques using zebrafinch brain sections, quite a departure from the electrophysiological work being performed in her lab. Allison is yet another example of how to do everything well: science, volleyball, cooking, and maintenance of a dilapidated car. I especially appreciate the help and friendship of Gabriella Cabrillo, the research associate in the lab. While my rotation project did not culminate in stellar results, despite assistance from the *in situ* maestro Alessandro Bulfone in John Rubenstein's lab, it did spark my interest in neuroscience and the potential of *in situ* hybridization techniques, which led me to the Rubenstein lab.

John Rubenstein was a bit hesitant to have a Master's student join the lab, but then consented. I have thoroughly enjoyed my time in the Rubenstein lab. Specifically, Jason Long, Sandy Chen, MengSheng Qiu, Kenji Shimamura, and Lori Sussel have been fonts of endless advice and friendship. I also need to thank Stewart Anderson, Phil Crossley, Marina Mione, and Kenji Shimamura for their expert assistance with the Adobe Photoshop program, thus saving me countless hours of frustration. John is a model to me of how to do good science yet have an outside life: how to cherish and enjoy your children, and how keep a sense of humor (albeit including bad jokes) while doing science.

This project would not have been possible without one final collaborative component: a neuroanatomy expert to help me interpret the complicated data. Comparison between mouse and chicken brains is difficult, as the appearances and even terminology differ considerably; therefore, I am extremely grateful for the expertise of Luis Puelles, in Murcia, Spain.

And towards the end of this project, my thesis committee of John Rubenstein, Allison Doupe, and Peter Ralston provided me with insightful feedback and the necessary stamp of approval.

Finally, I need to acknowledge the people closest to me. I would definitely not be in science if it weren't for my chemist parents. My parents have always been supportive of what I chose to do, for which I'm deeply grateful. And my husband, Luke Hoffman, another scientist in my life. He is the most supportive person I have ever met. We have known each other for a long time, yet it is always refreshing to find out that we can weather stressful times such as these, when we're both writing our theses and battling for the computer. I have never met anyone who is so generous with his time, energy, and talents.

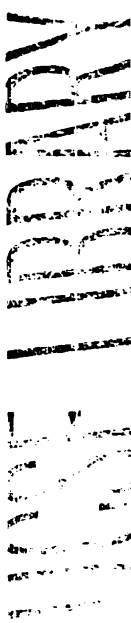

Table of Contents

List of Figures

List of Tables

List of Schemas

List of Appendices

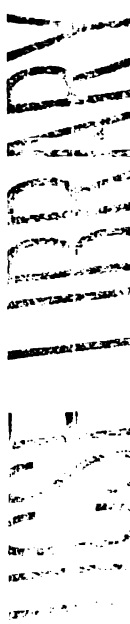

Glossary of Anatomical Terms

ACX	Archicortex
AEP	Anterior entopeduncular area
AH	Anterior hypothalamus
AS	Archistriatum
BNST	Bed nucleus stria terminalis
CB	Cerebellum
CH	Chorioid plexus
DB	Diagonal band
DLVR	Dorsolateral ventricular ridge
DT	Dorsal thalamus
DVR	Dorsal ventricular ridge
EMT	Eminentia thalami
EP	Epiphysis
ET	Epithalamus
FP	Floor plate
GV	Geniculatus ventralis nucleus
LA	Lateralis anterior nucleus
LFB	Lateral forebrain bundle
LGE	Lateral ganglionic eminence
LPO	Lobus parolfactorius
LT	Lamina terminalis
MA	Mammillary area
MGE	Medial ganglionic eminence
NCX	Neocortex
OB	Olfactory bulb

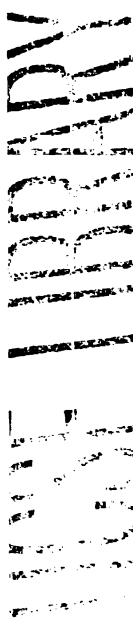

OR	Optic recess
OS	Optic stalk
PA	Paleostriatum augmentatum
PCX	Paleocortex
PEP	Posterior entopeduncular area
POA	Anterior preoptic area
POP	Posterior preoptic area
PP	Paleostriatum primitivum
PSP	Pallio-subpallial limit
PT	Pretectum
RCH	Retrochiasmatic area
RM	Retromammillary
RP	Roof plate
SE	Septum
SOC	Supraoptic commissure
SPV	Supraoptic/paraventricular area
SVZ	Subventricular zone
TR	Tractus retroflexus
TU	Tuberal hypothalamus
VL	Ventrolateralis nucleus
VT	Ventral thalamus
VZ	Ventricular zone
ZI	Zona incerta
ZL	Zona limitans

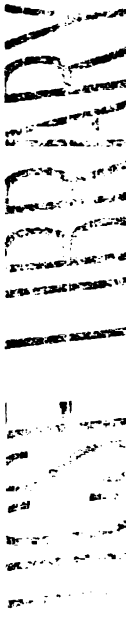

Introduction

Portions of this thesis are being adapted for inclusion into a manuscript by Kuwana, E., Puelles, L., Rubenstein, J.L.R., et al., to be submitted in 1997.

The central nervous system (CNS) is derived from the neural plate, a simple, single layer of neuroepithelial cells. Sequential inductive signals act on the neural plate to create regional molecular differences. These differences then regulate different programs that direct region-specific proliferation, migration, and differentiation within the CNS.

There are four main subdivisions of the CNS: the spinal cord, the hindbrain (rhombencephalon), the midbrain (mesencephalon), and the forebrain (prosencephalon). Of these subdivisions, it has been demonstrated that the hindbrain is organized in a segmental, or neuromeric (divided into neuronal segments), manner (Keynes and Krumlauf, 1994, reviewed by Krumlauf, 1993). Mapping gene expression in the hindbrain identified candidate regulatory genes that regulate formation and specification of the hindbrain segments, termed rhombomeres. Based on this evidence, it was a logical step to investigate whether gene expression patterns would provide evidence for a similar organization in the forebrain. Investigating the patterning of the vertebrate forebrain, however, is complicated by its highly complex topography. Although a neuromeric organization is not as readily apparent in the forebrain as that observed in the hindbrain, available evidence supports some degree of segmentation within the forebrain.

The subdivisions of the brain can be distinguished from each other in a multitude of ways, such as histologically, molecularly, or functionally. The forebrain can be identified functionally by its role in higher neurological and cognitive functions such as the processes of learning and language.

Olfactory and visual information, for example, are processed primarily in forebrain-derived tissues. The forebrain is subdivided into the diencephalon and the telencephalon. The diencephalon surrounds the 3rd ventricle and consists of the thalamus, hypothalamus, and epithalamus. The telencephalon expands into the cerebral hemispheres as it develops and is composed of the cerebral cortex, claustrum, hippocampus, olfactory bulbs and vesicles, and the basal ganglia: caudate, putamen, globus pallidus, and amygdala.

The cerebral cortex is largely responsible for higher cognitive functions. During evolution, the size and functional importance of the cerebral cortex has increased greatly with respect to the rest of the CNS, perhaps in order to accommodate higher cognitive tasks. Higher vertebrates such as primates have more surface area in the telencephalon as a result of the sulci and gyri that create folds on the cortical surface. Specifically, the neocortex (a mammal-specific hexalaminar cerebral cortical region) has grown disproportionately in higher mammals. In order to gain insight into the evolutionary origin of the neocortex, it is first imperative to understand how the neocortex, and the forebrain in general, are formed and organized. The cellular and molecular mechanisms that give rise to pattern formation and regional specification within the telencephalon (early in embryogenesis, the neural plate and neural tube) are still unclear. Therefore, more investigation is necessary to clarify the role of regulatory genes in regulating morphogenesis and differentiation within the forebrain.

The embryonic organization of the forebrain is not well understood. This study uses the expression of transcription factors encoding genes as an approach to compare the organization of the avian and mammalian embryonic forebrain. Several models have been suggested to address the

issue of forebrain organization. Although neuromeric boundaries are less obvious in the forebrain than in the hindbrain (Bulfone et al., 1993, 1995; Puelles and Rubenstein, 1993; Rubenstein et al., 1994; Alvarez-Bolado et al., 1995; Shimamura et al., 1995; Tole and Patterson, 1995), a theory called the prosomeric (prosencephalic neuromere) model has been posited (Puelles and Rubenstein, 1993). This theory states that morphological landmarks such as transverse constrictions in the neural tube, gene expression patterns, and anatomical data define longitudinal columns and transverse segments which, in turn, create molecularly distinct histogenic domains (Shimamura et al., 1995). For example, as shown in Shimamura et al., *Nkx-2.2* expression (another regulatory gene) and axonal tracts (as shown by alphaN-catenin protein) define the longitudinal axis. It is hypothesized that there are six prosomeres, which can be subdivided into diencephalic (p1 to p3) and secondary prosencephalic (p3 to p6) neuromeres. This model is further subdivided by the longitudinal reference lines of the roof, alar, basal, and floor plates of the spinal cord; each prosomere is divided into these longitudinal domains.

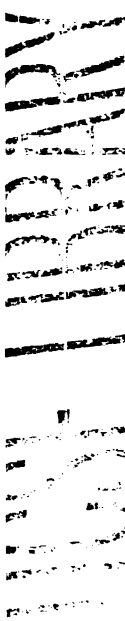

Many transcription factor encoding genes are candidates for regulating pattern formation and differentiation in the forebrain. These genes include homeobox (Boncinelli et al., 1995), paired domain (Bopp et al., 1986, Dressler et al., 1988), and helix-loop-helix (Murre et al., 1989) family members. Many of these genes are expressed in the embryonic forebrain with temporally and spatially restricted expression patterns; therefore, they are likely to contribute to the regional specification and histogenesis within these regions. Furthermore, mutational analyses have demonstrated that many of these genes play an important role in forebrain development (Ang, et al., 1996).

The genes chosen for this study are expressed at the early stages of embryogenesis in the ventricular zone (VZ, an area of proliferating, undifferentiated cells) and in the mantle zone (an area where cells are in the process of differentiating into glia and neurons). The early expression of these genes suggest that they regulate development before synaptic activity, such as thalamic connections, can influence forebrain organization (Bulfone et al., 1993; Alvarez-Bolado et al., 1995). The five genes were chosen on the basis of their restricted expression patterns; these markers have expression patterns that are predominantly exclusive of each other within regions of the forebrain.

Dlx-2 is a homeobox-containing gene which is a homologue of the *Drosophila* gene *distalless* (Porteus et al., 1991). *Dlx-2* encodes a putative transcription factor that is expressed in the embryonic basal telencephalon and part of the hypothalamus during neurogenesis. *Dlx-2* expression, however, is reduced in the adult brain.

Tbr-1 is a homologue of *Brachyury* (Bulfone et al., 1995). It is expressed in the post-mitotic cells of the telencephalon during embryogenesis and through adulthood.

Pax-6 (Walther and Gruss, 1991) was identified by its homology with the paired-box motif, a motif initially identified in *Drosophila* segmentation genes, such as *paired* (Bopp et al., 1986; Baumgartner et al., 1987). It encodes a transcription factor and is primarily expressed in the cortical compartment. It is expressed in the telencephalic vesicles and in the presumptive lens, cornea, and retina (Walther and Gruss, 1991).

Nkx-2.1, which was originally identified as *Thyroid Transcription Factor 1* (*TTF-1*), is homologous to the *Drosophila* gene *NK-2*, which is expressed in neuroblast precursor cells (Kim and Niremberg, 1989). *Nkx-2.1* is

expressed in the medial ganglionic eminence and in the ventral hypothalamus (Shimamura, et al., 1995).

Emx-1 is a homeobox-containing gene related to *empty spiracles* in *Drosphila,* which is expressed early in embryogenesis (Boncinelli, 1995). *Emx-1* expression is evident in the olfactory bulbs and in the ventricular zone of the cerebral cortex during cortical neurogenesis (Simeone, et al., 1992).

Previous comparative neuroanatomical studies have focused on the distribution of markers such as acetylcholinesterase (Puelles et al., 1986). Now that earlier markers are available, a comparison of homologous regions in different species can be made which relies upon an earlier, more primary influence of transcription-factor-encoding genes. This project compares the organization of the embryonic forebrain by comparing RNA transcript distribution at equivalent developmental timepoints in chicken and mouse tissues, with a primary focus on chicken forebrain development.

In more general terms, comparing the distribution of transcription factors in avian and mammalian brains can be used as a tool to investigate the organization of brain development. This approach also can be used to investigate whether genetic regulation of brain development differs between species. Avians and mammals function very differently; one sense, such as smell, that is vital to survival in one species may be of lesser importance to the other species. Thus, it is easy to imagine one part of the brain expanding over evolution to accommodate specialized functions. This is the assumption held for the area of the brain called the neocortex (neo- meaning new), an area thought to be unique to mammals. For this reason, it will be interesting to learn the genetic underpinnings of phylogenetic neuroanatomical differences in species as seemingly different as mammals and avians. Furthermore, this work will provide an anatomical foundation

for further neuroembryological experiments. Thus, this study aims to elucidate the genetic organization of the forebrain and to provide insight into its evolution.

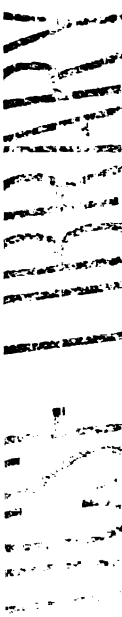

Background to Experimental Approach

In Situ Hybridization

In situ hybridization was developed initially as a way to localize specific DNA sequences on chromosomes (Gall et al., 1971). Now this highly sensitive method can be applied to detect and localize RNAs, even those of low abundance. There are two major types of *in situ* hybridization; one uses a radioactive ^{35}S probe, while the other uses a non-radioactive digoxigenin probe.

The first step to an effective *in situ* hybridization is proper tissue preparation: the tissue should be fixed in paraformaldehyde sufficiently to preserve cellular morphology, but not so much that probe access is hindered. The length of fixation has to be determined empirically based on the age, size, and permeability of tissue being processed.

One of the important prehybridization steps is permeabilization of the tissue to allow for probe access. This is accomplished by proteolytic digestion; again, as with fixation, this process must be carefully limited in order to maintain cellular morphology. An additional step of acetylation is often used to decrease background signal by minimizing non-specific hybridization.

Most probes are single-stranded RNA probes which have been transcribed from plasmids that have a T3, T7, or SP6 promoter.

Following the *in situ* hybridization, the signal is detected using autoradiography. Autoradiographic film is used to access quickly (overnight) whether the *in situ* hybridization worked; this method has low resolution. Next, the slides are dipped in autoradiographic emulsion, which detects

Materials and Methods

Preparation of Mouse Tissue

Mouse embryos were staged by considering the midday of the vaginal plug to be equivalent to embryonic day 0.5 (E0.5). Mouse E13.5 tissue was chosen for comparison to chick tissue because this stage of mouse development corresponds approximately to the stage of development between chick ages E10.5 and E14.5, which represents the age of peak expression for the genes included in this study. Mouse E13.5 embryos were isolated and the brains were fixed overnight in 4% paraformaldehyde in phosphate-buffered saline (PBS) with 4% sucrose added. After cryoprotection in sucrose solutions (10%, 20%, and 30% sucrose in 1x phosphate-buffered saline (PBS) until brain equilibrates and sinks), the brains were embedded in OCT embedding compound (Tissue-Tek) and sectioned at 20 μm thickness onto Superfrost Plus slides (Fisher Chemical Co.). Solutions and water were treated with diethylpyrocarbonate (DEPC) (Sigma Chemical Co.).

Preparation of Chick Tissue

Chick embryos were obtained from fertilized eggs from Feather Hill Farms and SPAFAS, Incorporated at embryonic day zero. Chick embryos from various stages were isolated and fixed as described above for mouse brains. At stage E5.0, the entire head and branchial arches were used. For stages E8.5, E10.5 and E14.5, the brains were dissected from the embryos. Embedding and sectioning were performed as described above.

Preparation of RNA probes

For all *in situ* hybridizations, riboprobes were prepared and synthesized as described previously (Zoeller at al., 1989) with a specific activity added per slide of 2 x 10^6 cpm. For details, see Table 1 and text below:

Table 1: Summary of Riboprobes

Mouse Riboprobes:

gene/(clone)	vector	insert size	reference/source	rest enz	RNA polym. /hydrolysis
Dlx-2 (E298-1)	pBS E61	1.7 kb	Porteus et al., 1991	EcoRI	T3
Tbr-1 (156A)	pBS E61	264 bp	Bulfone et al., 1995	HindIII	T3
Pax-6 (6sc32)	pBS KS$^-$	260 bp	Walther, Gruss, 1991	EcoRI	T3
Emx-1		900 bp	Qiu et al.,1996	EcoRI	T7
Nkx-2.1	pBS E61	2.1 kb	Shimamura et al., 1996	SalI	T3/25 minutes

Chick Riboprobes:

gene/(clone)	vector	insert size	reference/source	rest enz	RNA polym. /hydrolysis
Dlx-2 (1A3)		700 bp	J. Keleher	EcoRI	T7
Tbr-1 (1A1)		3.0 kb	A. Bulfone, S. Smiga	BamHI	T7
Pax-6 (3-4T)		1.3 kb	K. Yasuda	BspD1	T7
Emx-1	pGEM3	400 bp	E. Boncinelli	HindIII	T7
Nkx-2.1	pBS SK$^-$	2.0 kb	L. Sussel	EcoRI	T7/25 minutes

Details for Riboprobes

The mouse *Pax-6* cDNA was graciously provided by Walther and Gruss; the other mouse probes were isolated in the Rubenstein lab and details can be found in the reference cited in Table 1. The chick *Pax-6* cDNA was a generous gift of K. Yasuda; the chick *Emx-1* cDNA was kindly given to us by E. Boncinelli. Other chick probes were isolated in our lab and details (also listed in Table 1) are as follows:

Chick *Dlx-2* was isolated by J. Keleher from a chicken E10.5 cDNA library (courtesy of T.E. Kennedy) using low stringency hybridization and mouse probes. The *Dlx-2* in this study originated from clone 1A3. EcoRI and T7 were used to obtain a 700 bp probe.

Chick *Tbr-1* was isolated by A. Bulfone and S. Smiga from a chicken E10.5 cDNA library (courtesy of T.E. Kennedy) using low stringency hybridization and mouse probes, resulting in the identification of clone 1A1. BamHI and T7 were used to obtain a 3 kb probe.

Chicken *Nkx-2.1* was isolated by L. Sussel from a chicken E10.5 cDNA library (courtesy of T.E. Kennedy) using a portion of the mouse *Nkx-2.1* cDNA as a probe. EcoRI and T7 were used to obtain a 2 kb probe that required 25 minutes of alkaline hydrolysis (for details see Appendix IV) (L. Sussel, unpublished results).

The general molecular biological techniques used are described in Molecular Cloning, A Laboratory Manual, 2nd edition by Sambrook et al., Cold Spring Harbor Laboratory Press, 1989.

In situ RNA Hybridization in Tissue Sections

RNA probes were transcribed with the appropriate RNA polymerase in the presence of ^{35}S UTP (NEN Radioactive Nucleotides). *In situ* hybridization was performed on adjacent sections, as noted in the figure

legend for each composite figure. The sections shown in a composite figure represent tissue from a single embryo. For each probe, sections were processed, prehybridized, hybridized, and washed (Bulfone et al., 1993b). Solutions and water were treated with diethyl pyrocarbonate (DEPC) (Sigma Chemical Co.) and all glassware was baked at 230° Celsius for 6-8 hours.

Slides were then coated with Kodak NTB-2 (Eastman Kodak Co.) photographic emulsion diluted 1:1 with distilled water with 1% glycerol added. The brain sections were exposed 10-14 days depending on the strength of signal shown by overnight exposure to autoradiography film (Hyperfilm-MP, Amersham). The exposed slides were developed in Kodak D-19 developer diluted 1:1 with distilled water, fixer (Eastman Kodak Co.), and tap water. The sections were stained with toluidine blue (0.1%) containing 10 mM sodium acetate at pH 4.7 for histological identification. After the sections were processed through ethanol dehydration, coverslips were mounted with Permount histological mounting medium (Fisher Chemical Co.). Slides were examined using both dark- and bright-field illumination. An Olympus SZH-10 series research zoom stereo microscope was used for tissue isolation and for photographic purposes.

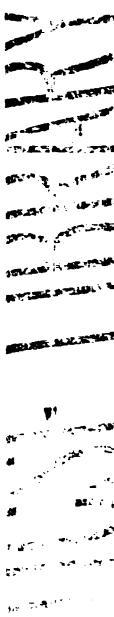

Scanning and Adobe Photoshop Processing

Photographic negatives, emulsion side down, were scanned using a 35 mm Film Scanner LS-1000 and Strip Film Holder FH-2 (Nikon Corp.). Adobe Photoshop, Macintosh version 3.0 (Adobe Systems Incorporated), was used for the brightness and contrast corrections on digitized images that were then used to build composite figures.

Results for Mouse *In Situ* Hybridizations

Mouse Pattern at E13.5

The results presented here are complementary to previously published gene expression patterns for *Dlx-2* (Bulfone et al., 1993), *Tbr-1* (Bulfone et al., 1995), *Pax-6* (Stoykova and Gruss, 1994) and *Emx-1* (Simeone et al., 1992). In the E13.5 mouse brain, the less obvious telencephalic components (claustrum, amygdala, and bed nucleus stria terminalis (BNST)) can be distinguished with more confidence than in earlier stages of mouse development. The following descriptions are based on alternate successive sections in the horizontal plane, hybridized correlatively with the various probes. The gene *Nkx-2.1* was included in this particular study, but because gene expression data for *Nkx-2.1* were previously published, a separate analysis for this gene was not provided in this study (Price et al., 1992).

The plane of section is approximately horizontal; previously published results provide gene expression patterns in the coronal plane of section.

Areas of the Pallium and Subpallium:

Dlx-2 is strongly expressed in the ventricular zone (VZ) and in the subventricular zone (SVZ) of the lateral ganglionic eminence (LGE) and the medial ganglionic eminence (MGE). There is also signal in the mantle zone of the LGE and MGE, although *Dlx-2* expression here is weaker than in the VZ and SVZ (Figs. 1g and k). The pallial-subpallial (PSP) boundary is clearly defined by *Dlx-2* expression. Additionally, *Nkx-2.1* is expressed in the VZ and mantle zone of the MGE, but not in the LGE; this provides an easy distinction between the two eminences (not shown, see Price et al., 1992 and Shimamura et al., 1995). More caudal to the LGE and ventral to cortex, *Dlx-2* is expressed

in the BNST and in the central part of the amygdala (Fig. 1o). The amygdaloid complex shows *Dlx-2*, *Tbr-1*, *Pax-6*, and *Emx-1* signal (Figs. 1m, n, o, p, and data not shown).

The *Tbr-1* probe serves as a marker for pallial (cortical) structures in the mouse telencephalon (Bulfone et al., 1995); its signal appears restricted to the mantle zone throughout the cortex and the claustrum (Figs. 1e, i, and m). *Tbr-1* has a weaker intensity of expression in the area of the claustrum than in the cortex and there is a sharp boundary of signal at the PSP limit.

Pax-6 expression appears restricted to the pallial VZ (Stoykova and Gruss, 1994), but signal appears as well in a band of mantle cells that are intercalcated between the claustrum and the striatal primordium (Figs. 1f, j, and n). This latter group of cells apparently overlaps with the most lateral part of the striatal mantle and extends from the pallial ventricular sulcus to the olfactory tuberculum; intensely labeled cells occupy the brain surface here. Additionally, *Pax-6* also is expressed weakly within the VZ (pseudostratified epithelium) and SVZ of the LGE (Figs. 1f and j).

In contrast, the *Emx-1* probe is strictly a cortical marker (Simeone et al., 1992). Its expression appears in cortical VZ and mantle zone and extends homogeneously over the primordia of the hippocampal cortex, neocortex, and olfactory paleocortex. Its expression does not, however, overlap with the claustrum, as defined by *Tbr-1* expression (Figs. 1e, i, and m). *Emx-1* signal is present in the mantle layer of the lateral amygdala, whereas the VZ is largely negative. In contrast, *Tbr-1* signal is strong in the prospective medial and cortical portions of the mantle zone of the amygdala. The *Pax-6* signal is restricted to the VZ, although it does slightly overlap the *Dlx-2* positive area, which extends well into the SVZ and mantle layers of the amygdala.

The olfactory bulb displays *Pax-6* expression in the VZ, *Dlx-2* in the SVZ, and both *Tbr-1* and *Emx-1* in the mantle zone (data not shown).

Telencephalic Stalk Area:

Tbr-1 is expressed in cells of the diagonal band in both the vertical and horizontal limbs. It also appears to be in the thin superficial cellular layer at the olfactory tuberculum (Figs. 1e, i, and data not shown) and at the septum. In comparison, *Pax-6* labels the superficial olfactory tuberculum and septal cells. In the septal SVZ and adjacent mantle zone *Dlx-2* signal is apparent.

The eminentia thalami (EMT) expresses *Pax-6* in the VZ, with maximal intensity seen close to the telencephalic choroidal plexus (Figs. 1j and n). This marker appears in the more ventrally placed mantle cells of the bed nucleus stria medullaris (Fig. 1g). In contrast, *Tbr-1* intensely labels the whole mantle of the EMT (Figs. 1e, i, and m) in a characteristic comma-shaped formation. This forms the caudal wall of the foramen Monroi and is well delimited caudally from the ventral thalamus, as labeled by *Pax-6*, *Tbr-1*, and *Dlx-2* expression (Figs. 1i, j, and k). In the sections from the level of the mutual crossing of the internal capsule and the stria terminalis, the *Tbr-1* domain shows a clear boundary with the *Dlx-2* positive BNST (Fig. 1g) and connects laterally with the end of the hippocampal formation, just medial to the amygdala (Figs. 1k and o). At the transition of the EMT into the bed nucleus of the stria medullaris outside the telencephalon, there appears to be a superficial band of *Tbr-1* positive cells which connects the eminential area to the horizontal limb of the diagonal band (Figs. 1i and m). This might represent a primordium of the magnocellular preoptic nucleus, as it relates medially with the *Dlx-2* positive domain of the preoptic region (Fig. 1o).

Table 2: Summary of Results

Mouse Expression Pattern

Structure/Area	Genes Expressed
Pallium: Neocortex	*Emx-1*, *Tbr-1*, and *Pax-6*
Pallium: Archicortex	*Emx-1*, *Tbr-1* (weak), and *Pax-6*
Pallium: Paleocortex	*Emx-1*, *Tbr-1*, and *Pax-6*
Claustrum	*Tbr-1*
Striatum	*Dlx-2* and *Pax-6* (weak)
Pallidum	*Dlx-2* and *Nkx-2.1*

Chicken Expression Pattern*

Structure/Area	Genes in VZ	Genes in Mantle
Pallium: DVR, Wulst	*Pax-6* and *Emx-1*	*Tbr-1*
Claustrum	*Tbr-1*	*Tbr-1*
Striatum	*Dlx-2* and *Pax-6* (weak)	*Dlx-2*, *Pax-6*, and *Nkx-2.1*
Pallidum	*Nkx-2.1* and *Dlx-2*	*Nkx-2.1* and *Dlx-2*

*as judged from ages of peak expression: E10.5 and E14.5

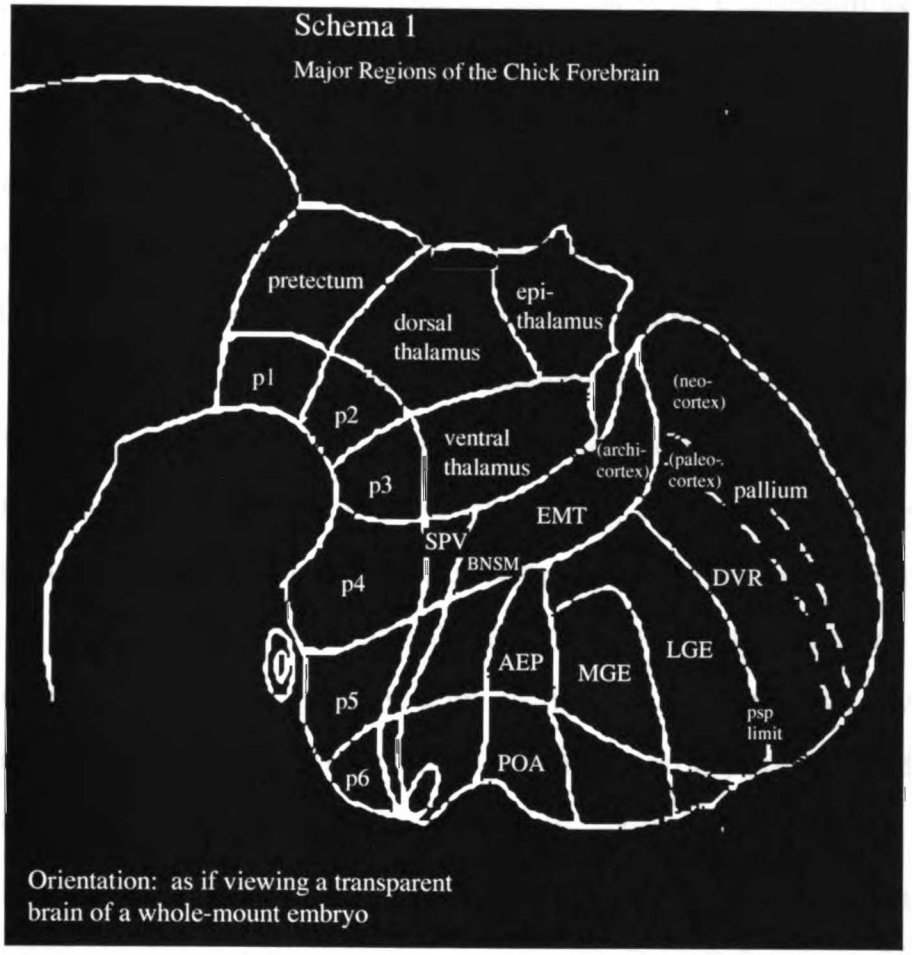
Schema 1
Major Regions of the Chick Forebrain
pretectum
dorsal thalamus
epi-thalamus
p1
p2
p3
p4
p5
p6
ventral thalamus
(archi-cortex)
(neo-cortex)
(paleo-cortex)
pallium
EMT
SPV
BNSM
DVR
AEP
MGE
LGE
POA
psp limit
Orientation: as if viewing a transparent brain of a whole-mount embryo

Results for Chicken *In Situ* Hybridizations

Most of this analysis focuses on coronal sections, as the histological and morphological quality are superior to that seen in the sagittal sections. The sagittal data are used predominantly to complement and support the conclusions drawn from the coronal sections. The expression observed in the eye region is an artifact unless noted.

In the E5.0 sections, there are two "basal" protrusions in the rostral coronal sections (Fig. 2a-d) which most likely represent the primordia of the lateral ganglionic eminence (LGE) and the medial ganglionic eminence (MGE). The pallium and lamina terminalis adjoin this region.

In the E8.5 sections, the large nuclear area below the pallial-subpallial (PSP) limit (as defined by *Tbr-1* and *Dlx-2* expression patterns in Fig. 5e and f) corresponds to the true striatum, comprising confirmed homologues in mammals of the nucleus caudoputamen and the nucleus accumbens.

In the E10.5 sections, the shape of the coronal sections are becoming more amenable to comparison with sections from equivalent levels in the adult chick brain. This facilitates comparisons with published adult chick brain atlases, thus enabling one to identify structures with more confidence.

In the E14.5 sections, structures are more differentiated and subdivisions are apparent within previously identified areas. Also, the relative areas of the eminences and striatum have expanded greatly, and as such, the expression patterns are in wide bands, facilitating mapping of boundaries.

Expression Patterns at E5.0 and E8.5

Dlx-2

At E5.0, in the rostral coronal sections (Fig. 2a-d), the lamina terminalis, MGE, and LGE express *Dlx-2* with a sharp boundary at the PSP limit (Figs. 2b and f; 3b and e; 4b, f, and j). *Dlx-2* signal in these areas is limited to the transition between the ventricular ridge and the mantle zone, labeling only the deepest differentiating neurons. The *Dlx-2* domains in the MGE and LGE show drastically different radial dimensions (Figs. 2f; 4f): in the LGE, the majority of signal is restricted to the periventricular cells; in contrast, the MGE's cell lamina next to the ventricular zone (VZ) displays a strong *Dlx-2* signal. The more superficial cells in the MGE show a less intense signal. The MGE primordia thins medially into the rostral preoptic area next to the median lamina terminalis, which is narrow and becomes *Dlx-2* negative more caudally (Figs. 2f; 4f). In the anterior preoptic region, only *Dlx-2* signal is evident. *Dlx-2* is negative in the optoeminential domain but positive in the postoptic strip that extends toward the median chiasmatic area (Fig. 3e). The ventral thalamus (VT), a triangular area rostral to the zona limitans (ZL), is *Dlx-2* positive. The maxillary process of the branchial arches, the mandibullary process, and the hyoid arch (Figs. 2f; 3b and e) express *Dlx-2*.

At E8.5, the large nuclear area below the PSP limit (Fig. 5e and f) corresponds to the true striatum. *Dlx-2* signal is in this entire area, periventricularly and extending into the deeper stratum of the striatal primordia (Figs. 5f; 6c). More caudally in the hemisphere, there is expression at the transition between the preoptic and peduncular areas (Figs. 5f and data not shown). This labeled thicker periventricular stratum still represents the striatal primordia, namely the MGE. The labeled thinner periventricular stratum below corresponds to the round lateral forebrain bundle (LFB); this bundle enters the telencephalon laterally and corresponds to the pallidal homologue: the MGE, and possibly the anterior entopeduncular area (AEP).

Dlx-2 expression is continuous deep to the LFB (Fig. 5l and data not shown), rostral to the zona incerta (ZI).

Outside of the telencephalon, the alar plate shows a clear caudal boundary of expression that corresponds to the ZL (Fig. 6c and data not shown). The ventral thalamus is rostral to the ZL and is comprised of two portions. There is an intensely labeled VZ that forms a triangular-shaped ventricular recess (termed the pseudosulcus parencephalicus by Kuhlenbeck). There also is a less markedly positive mantle layer that builds the primordia of several nuclei: the lateralis anterior (LA) dorsal to the ventricular recess; the geniculatus ventralis (GV) ventral to the recess; and the zona incerta (ZI) ventral to the recess (Figs. 6a-e and data not shown). There is *Dlx-2* signal in the supraoptic/paraventricular area (SPV) and in the posterior peduncular area (PEP) that extends behind the preoptic recess, in front of the negative juxtaoptic tract (also called the postoptic commissure) and into the chiasmatic area (Figs. 6a-e and data not shown). The SPV is a negative periventricular patch surrounded by a thin shell of *Dlx-2* positive cells. From here, *Dlx-2* expression extends into the tuberal hypothalamic recess, leaving the mammillary region negative (data not shown). Also, the anterior olfactory bulb is *Dlx-2* negative. This *Dlx-2* pattern, with a few minor exceptions that require further clarification, clearly reproduces the mouse pattern. These areas that need further analysis are olfactory bulb (OB) expression patterns and *Dlx-2* expression in the dorsal ventricular ridge, which appears to be in the posterior part of the DVR, which is strange because this area is *Tbr-1* positive (Figs. 6b, c, and data not shown) and should have no *Dlx-2* signal.

Tbr-1

At E5.0 in the rostral coronal sections, the mantle layer, which forms a thicker stratum in the pallium than in the ganglionic primordia, expresses *Tbr-1* (Figs. 2d and h; 3d and g; 4d, h, and l). The pallial mantle diminishes in thickness towards the medial roof tissue (prospective choroidal plexus, which is *Tbr-1* negative). In a pattern similar to the *Dlx-2* pattern, there is a sharp boundary laterally at the PSP. It appears that the presumptive LGE has fewer *Tbr-1* positive cells in its mantle than the MGE; however, the median area of the lamina terminalis is negative. As is apparent with *Dlx-2*, *Tbr-1* expression patterns define separate superficial cell groups in the MGE and LGE (Figs. 2h; 4h). At the most caudal end of the MGE and LGE (delineated by *Dlx-2* expression in Fig. 3f), a similar level of expression in the mantle of the pallium, LGE, and MGE is evident that stops sharply at the boundary of the MGE with the AEP and preoptic region. This boundary area is *Tbr-1* negative (Fig. 3d). Thus, *Dlx-2* and *Tbr-1* expression patterns demarcate the boundary of the MGE with the AEP and EMT (Fig. 3b, d, and e). At the median plate, *Dlx-2* and *Tbr-1* expression patterns are complementary (Fig. 3e, g): the lamina terminalis is *Dlx-2* positive up to the prospective anterior commissure, and the rest of the commissural median up to the choroidal roof is *Tbr-1* positive. The pallial domain shows continuity of *Tbr-1* signal across the presumptive amygdaloid area into the eminentia thalami region (EMT) (Figs. 3d, e, and data not shown); this is consistent with mouse data. The most dorsal aspect of the EMT labels with *Tbr-1* (Fig. 3d). No signal is visible caudal to this.

In the telencephalon at E8.5, the pallial *Tbr-1* domain has developed significantly, now covering distinct cortical and nuclear portions (Figs. 5c and e; 6a and b). This encompasses all cortical areas: medial, dorsomedial, dorsal, dorsolateral, lateral, caudal and caudoventral. Curiously, cells expressing *Tbr-*

1 in the pallium now are concentrated in the deeper mantle layer, and are covered homogeneously by a superficial layer of negative cells. There is a change in the mantle zone thickness from the prospective corticoid region (modified cortex with hidden lamination) to the much thicker DVR primordium.

Near the PSP boundary (later the lamina medullaris dorsalis), a gap parallel to the brain surface is relatively *Tbr-1* negative and serves to separate the most superficial *Tbr-1* positive cells from the deeper large cell mass (assumed to be *Tbr-1* negative) (Fig. 5e). *Tbr-1* is expressed only at the surface of the true striatum, labeling an irregular sheet of neurons that disperses in a graded manner into striatal and septal primordia. There is more *Tbr-1* expression in the septum than in the striatum; the septal *Tbr-1* positive cells seem to be restricted to the surface septal area, which is *Dlx-2* negative (Fig. 5f).

The *Tbr-1* pattern shows a clear rostrocaudal gradient in the cortical pallium (Fig. 6b and data not shown). *Tbr-1* label also covers the olfactory bulb (data not shown). As the sections progress, the PSP boundary curves more and more; at its caudal end is the transition into the EMT complex that just overlies the LFB. Below this are the dispersed *Tbr-1* positive AEP cells that connect rostrally with other positive cells near the brain surface; these cells may represent part of the diagonal band complex. Some of these positive cells at the surface may correlate with a stratum covering the pallidum or MGE. More caudally, the telencephalic peduncle at the level of the optic chiasma expresses *Tbr-1* (compare Fig. 5e with 6b). Caudal poles of the hemispheres show labeled cortical and archistriatal portions. The nuclear complex of the EMT that lies directly caudal to the unlabeled LFB labels strongly; this complex ascends ventrodorsally (Fig. 5e and data not shown).

Pax-6

Pax-6 expression in the E5.0 rostral coronal sections dominates the pallial neuroepithelium (Figs. 2c and g; 3c and g; 4c and g) and extends past the PSP ridge into the LGE, thus partially overlapping *Dlx-2* territory. There is a decreasing gradient of signal into the LGE area. The pallium does not appear to have *Pax-6* positive cells in the mantle layer. Moreover, *Pax-6* signal is evident in the EMT near the roof choroidal areas and in the neural retina, as well as in the caudal pallium, amygdaloid anlage, and ventral thalamus (Figs. 2g; 3f; 4g, k, and data not shown).

In the eye, *Pax-6* is in the anterior and equatorial epithelium of the lens primordium (Figs. 2g; 3c and f). The *Pax-6* signal shows an increasing ventrodorsal gradient of signal across the dorsal thalamus (DT) and epithalamus (ET) (data not shown). This gradient of expression ends at the epiphyseal bud, the primordium of the pineal gland at the roof.

Additionally, there is a group of differentiating neurons that are brightly *Pax-6* positive (there is a change of *Pax-6* pattern from the alar region into the basal region in the more caudal sections; data not shown). The hypothalamus is clearly separated into two portions: a negative p4 (mammillary) part and a *Pax-6* positive p5 (tuberal) part (Figs. 5h and i; 6e). The epithalamic anlage of the prospective habenular nuclei, which neighbors the dorsal choroidal tissue at the roof, exhibits maximal levels of *Pax-6*. Rathke's pouch, the adenohypophyseal anlage, also is positive (data not shown).

Pax-6 expression at E8.5 is similar to that seen in the E5.0 sections (Figs. 5d, h, i, and m). In the telencephalon, signal extends continuously throughout the whole pallial VZ, representing cortex plus the DVR, with

expression overlapping *Dlx-2* areas near the PSP boundary (Figs. 5d; 6e). There is still a decreasing gradient of expression into the VZ of the LGE. There is a curved area parallel to the PSP boundary where *Pax-6* expression overlaps *Dlx-2* signal.

The pallial mantle zone cells, however, remain negative. *Pax-6* positive cells are most abundant next to the PSP limit at the intermediate radial levels and deep levels toward the LFB; this pattern is analogous to the *Tbr-1* pattern seen more caudally at the EMT (Fig. 5i and data not shown). In contrast, interstitial *Pax-6* positive cells seem to respect the superficial region occupied by *Tbr-1* positive cells, in agreement with the E5.0 ISH data. Note that the dispersed neurons that cross the LFB area are uniformly *Pax-6* negative. (See Discussion for more details.)

Comparison to the *Dlx-2* signal suggests that the *Pax-6* signal is weak or absent in laterally placed ventral thalamic nuclei (Fig. 6e and data not shown) such as LA and GV. The deeper lying nuclei such as VL and ZI express *Pax- 6,* and this expression extends into the EMT and SPV (Fig. 7m). The VZ of the optoeminential domain, which is the upper part of the preoptic recess, seems to be labeled throughout (Fig. 6e and data not shown).

Another interesting aspect of the *Pax-6* expression pattern includes a surface layer of intensely labeled cells immediately caudal to the pineal stalk; this corresponds to a relatively unknown dorsal thalamic primordium. This area was identified as a layer of cells coming from a proliferative source near the dorsal midline (doctoral thesis by Guillen, Puelles lab, unpublished results). These cells migrate rostrally over the dorsal thalamic deep cell mass to build the anlage of the nucleus superficialis parvocellularis.

Nkx-2.1

At E5.0, *Nkx-2.1* expression is limited rostrally to the primordia of the MGE, seen as a band of signal in the medial portion of the section (Fig. 2a). As the section level progresses more caudally, there is expression in the VZ and mantle zone of the MGE (Figs. 2e; 3a; 4e), as well as in the hypothalamus (Fig. 4i) Comparison of *Nkx-2.1* expression pattern with that of the other markers shows an overlap with *Dlx-2* expression in the MGE area (Figs. 2a and e; 3a and e; Fig. 4e and f), although *Dlx-2* expression in this area is more restricted to the VZ. *Nkx-2.1* expression in the MGE is complementary to that of *Pax-6* and *Tbr-1* (compare Fig. 2a with 2c and d; Fig. 2e with 2g and h; Fig. 3a with 3c, f, d, and g; Fig. 4e with 4g and h), with a sharp demarcation at the PSP limit.

At E8.5, the *Nkx-2.1* expression pattern looks similar to that observed at age E5.0, although the various structures are becoming more differentiated. *Nkx-2.1* signal is evident in the VZ and mantle zone of the MGE (Figs. 5g; 6d), with expression persisting in the hypothalamus (Fig. 6d) The sharp boundary at the PSP limit is clearly visible. There is still overlap with *Dlx-2* expression in the ventral medial regions (Fig. 5f) and overlap with *Pax-6* in the ventral lateral regions.

Expression Patterns at E10.5 and E14.5

Dlx-2

Dlx-2 expression in the rostral sections is not very visible because the plane of section does not include the eminences yet (Fig. 9d). More caudally, however, there is clear expression in the VZ and mantle zone of the LGE and its striatal derivatives (Figs. 9i and n). Expression extends dorsally to the PSP limit, ending at the starting point of *Pax-6* and *Tbr-1* expression. At E14.5, *Dlx-2* is strongly expressed in the VZ with limited expression in the mantle zone of the striatum. *Dlx-2* expression also expands laterally, creating an area of

overlap with *Pax-6* expression (Fig. 10c) below the PSP limit. There is also expression dorsally in the septum. Viewed sagittally, there is expression in the LGE and preoptic areas Figs. 11c and g).

Tbr-1

The *Tbr-1* expression pattern at mid-gestation is similar to that seen at earlier stages. At E10.5, signal is visible in the VZ and mantle of the pallial regions (Fig. 9b, g, and l). This cortical marker ends abruptly at the PSP boundary. There is a slight overlap with *Pax-6* and *Emx-1* in the VZ of this region (compare Fig. 9g with i), but it is precisely complementary to the *Dlx-2* expression pattern. As the sections progress caudally, there is a band of *Tbr-1* negative cells dorsal to the *Tbr-1* positive VZ in the hyperstriatal region. At E14.5, *Tbr-1* has a large region of expression in the pallium, as the mantle has thickened and the area between the VZ and the pia has increased considerably (Fig. 10a). In sagittal sections, there is expression in the olfactory bulbs, pallial regions, and the vertical limb of the diagonal band (Figs. 11a and e).

Pax-6

Pax-6 expression is in the VZ of the pallium near the PSP boundary. A swath of *Pax-6* positive cells is visible from the VZ extending ventrally into the striatal region (Figs. 9h and m). There is a circular area that is *Pax-6* negative; this area is hypothesized to be the internal capsule area, where fibers traverse through the striatum. *Pax-6* expression forms a ring-shaped pattern of expression around this area. There is also expression on the surface of the LGE (Fig. 9m). *Pax-6* expression at E14.5 is similar to that noted at E10.5. At a caudal level, the coronal section captures all three components: the MGE, LGE, and pallium. *Pax-6* signal is apparent in the striatal cells, which form a

border around the large negative region in the middle. In this border, there is an area of strong signal just below the PSP limit (Fig. 10b). Sagittal section reveal expression in the olfactory bulbs, striatum near the PSP limit, and in the VT, the most caudal *Pax-6* positive structure (Fig. 11b and f).

Nkx-2.1

The sections probed with *Nkx-2.1* have a higher background, so only the most obvious signal was analyzed. At E10.5, *Nkx-2.1* signal is in the regions of the MGE and hypothalamus (Figs. 9j and o; Fig. 8f); a nested gene pattern can be viewed in Fig. 8 where *Nkx-2.1* in the MGE constitutes the inner-most area of expression in the sagittal sections.

At E14.5, *Nkx-2.1* expression mirrors that seen at E10.5: positive cells are in the MGE-derived cells in the striatum, with expression ventrally in the septal area (Figs. 10d; 11d; 9j and o). *Nkx-2.1* expression is also in the hypothalamus, with some expression visible in the olfactory bulb (Fig. 11d). All results listed here are consistent with expression patterns seen in mouse, with the possible exception of Nkx-2.1 expression in the olfactory bulbs.

At E14.5 in sagittal sections, *Nkx-2.1* is evident in the olfactory bulbs and the MGE (Fig. 11d); as with the other *Nkx-2.1* sections, the background level is relatively high, making the analysis of the true signal more obscure. More caudally in these sagittal sections, *Nkx-2.1* appears to be in the pallial region of the DVR; this structure has two levels of *Nkx-2.1* expression. The more anterior part shows a relatively weaker signal and the posterior region appears to have a stronger signal. This could be due to differences in cell density.

Emx-1

This gene was the last gene to be added to this study; as such, data are not available for all timepoints with this probe. *Emx-1* is expressed in the pallium in proliferating and postmitotic cells. At age E10.5, *Emx-1* is in the dorsal VZ of the pallium, with no expression detectable in the mantle zone (Figs. 9a, f, and k). Thus, *Emx-1* expression is limited to a narrow band of signal; it has the most restricted expression pattern of any of the genes analyzed. The VZ is a cell-dense area, and as such the *Emx-1* signal appears very bright in this area (Figs. 9a, f, and k). The *Emx-1* domain of expression in the VZ overlaps with *Pax-6* expression in the VZ. This borders upon the pallial domain of strong *Tbr-1* expression, although *Tbr-1* is expressed in the mantle zone, not the VZ. It looks as though Emx-1 expression overlaps with *Nkx-2.1* signal in the dorsal VZ, but this is an artifact of high background for the *Nkx-2.1* label. Therefore, of the genes included in this study, only the *Pax-6* signal overlaps with *Emx-1* expression.

Sagittal expression at E10.5

Viewed sagittally at E10.5, these genes create a nested pattern of expression: at the core of this pattern is *Nkx-2.1* in the MGE (Fig. 8f); outside of that is *Pax-6* signal, which overlaps some with the *Dlx-2* label; the third layer from the interior is *Dlx-2* expression, which is complementary to *Tbr-1*, the final, outer layer. *Tbr-1* has the broadest band of expression, filling the pallium as viewed sagittally.

Schema 2: Summary of Gene Expression Patterns

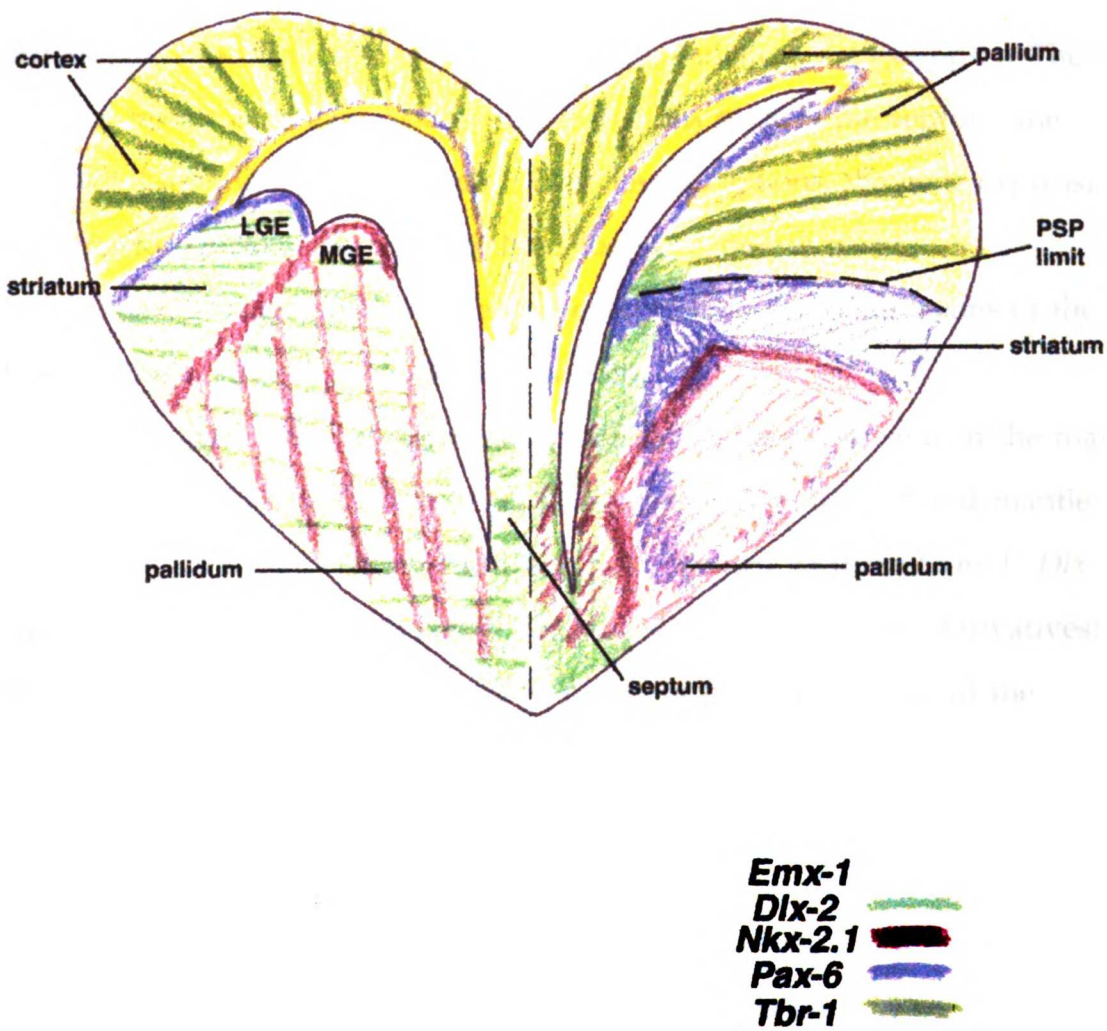

Conclusions

As presented in the Results section, each of the genes analyzed: *Dlx-2, Tbr-1, Pax-6, Nkx-2.1,* and *Emx-1* is expressed in a unique pattern in the embryonic forebrain. Area of gene expression overlap may represent a site of differential specification of some neuronal population, for example. These areas of mixed gene expression occur in regions such as the septum, the olfactory bulbs, and the amygdala. With few exceptions, the gene expression patterns for chicken recapitulate those found in mouse tissue.

For a listing of which genes are expressed in the subdivisions of the forebrain, see Table 2 in the Results section.

In general, *Dlx-2* is expressed in the ventricular zone and in the mantle zone of the pallidum; there is also *Dlx-2* expression in the VZ and mantle zone of the striatum. This pattern is complementary to that of *Tbr-1. Dlx-2* signal overlaps with that of *Nkx-2.1* signal in the MGE and its derivatives; there is also some overlap with *Pax-6* signal in the mantle zone of the striatum. There is, however, no overlap with *Emx-1* label. There is also *Dlx-2* expression in the ventral thalamus (VT) and in the supraoptic/paraventricular area (SPV).

Tbr-1 is expressed in the mantle zone of the pallium. *Tbr-1* expression stops abruptly at the PSP limit; its expression is complementary to that of *Dlx-2. Tbr-1* expression in the mantle zone of the pallium neighbors *Pax-6* and *Emx-1* expression in the VZ of the same region. *Tbr-1* expression does not overlap with *Nkx-2.1* signal. *Tbr-1* signal is also in the dorsal EMT, OB, and in the AEP. Most notably, *Tbr-1* is the only gene expressed in the claustrum, a pallial area between the striatum (LGE) and the lateral cortex. The

mammalian claustrum is thought to correspond to the avian DVR, as defined by *Tbr-1* expression.

Pax-6 labels the mantle zone (and the VZ weakly) of the striatum. In the pallium, there is *Pax-6* expression in the VZ which overlaps with *Emx-1* signal; nearby *Tbr-1* signal is evident in the mantle zone of this area. *Pax-6* labels the medial portion of the PSP limit; this expression overlaps with *Dlx-2* signal in the mantle zone of the LGE/striatum. *Pax-6* signal is excluded from the *Nkx-2.1* positive region in the MGE at early stages (e.g. E5.0), but at later stages *Pax-6* in the striatum overlaps with *Nkx-2.1* positive striatal cells in the region surrounding the internal capsule. There is also *Pax-6* signal seen in the VT and in the p5 tuberal portion of the hypothalamus. *Pax-6* signal also is in the eye region, specifically in the neural retina and lens primordium.

Nkx-2.1 expression is evident in the VZ and mantle zone of the pallidal region, labeling the MGE and its derivatives. This expression is localized with *Dlx-2* expression in both the VZ and mantle zone, although there is more Dlx-2 signal apparent in the VZ. At later stages, such as E8.5, some *Nkx-2.1* overlap with Pax-6 expression is apparent. This overlap is in the mantle zone of the striatum. There is no overlap of *Nkx-2.1* expression with *Tbr-1* or *Emx-1* signal. *Nkx-2.1* signal is also evident in the hypothalamus.

Emx-1 label displays the most restricted pattern of expression, labeling only the VZ of the pallium. This signal overlaps with *Pax-6* and runs parallel to *Tbr-1* expression in the mantle zone. *Emx-1* expression in the VZ is from the medial portion of the dorsal pallium to the lateral edge of the VZ, stopping abruptly while still in the pallial region, whereas *Pax-6* VZ expression continues ventrally, extending past the PSP limit.

Therefore, each gene has a unique expression pattern within the forebrain, as presented in more detail in the Results section. Some areas, however, require further clarification or discussion in order to address interesting gene expression patterns or to clarify areas of unexpected overlap.

Dlx-2 and *Tbr-1* expression patterns demarcate the boundary of the MGE with the AEP and EMT (Fig. 3b, d, and e). At the median plate, *Dlx-2* and *Tbr-1* expression patterns are complementary (Fig. 3e, g): the lamina terminalis is *Dlx-2* positive up to the prospective anterior commissure, and the rest of the commissural median up to the choroidal roof is *Tbr-1* positive.

At E8.5, there was an apparent discrepancy of overlap of *Dlx-2* and *Tbr-1* across the PSP limit. This needs further exploration and correlation with the coronal data in order to clarify this result. The question remains as to whether *Dlx-2* extends from the striatum into overlying posterior DVR territory in (Fig. 5f). There is a faint suggestion of a thin periventricular strip of *Dlx-2* positive cells, but further, more focused analysis is needed. This may provide clues about whether the DVR is a potential homologue for the claustrum, as opposed to the amygdala.

At E8.5, *Tbr-1* expression in the pallium is concentrated in the deep mantle layer with a superficial covering of *Tbr-1* negative cells. As no detailed autoradiographic study about the layering mechanism of the avian cortex is available, it is impossible to say whether the earlier cells remain positive and negative cells overlay them later, or if the initial expression is transitory so that the observed signal actually represents the young postmitotic cells just exiting the VZ.

At E8.5, also in the pallial mantle zone, there are cells that are *Pax-6* negative. It appears that postmitotic neurons migrate and become distributed

in variable numbers throughout the striatal primordium in the shell region that surrounds the core where the LFB traverses (internal capsule region). Neurons that cross the LFB are consistently *Pax-6* negative. This suggests that the *Pax-6* cells invade this primordium after the LFB is in place and subsequently fail to enter this core region. Curiously, these *Pax-6* positive cells do not extend across the accumbens into the septum (Fig. 5h), or more caudally into the pallidal complex (Fig. 5i and data not shown). These cells appear to respect the periventricular stratum that covers the *Pax-6* negative striatal VZ.

Another possibility to consider when trying to understand this interesting *Pax-6* pattern in the striatum is that the negative "core" region may contain postmitotic neurons derived from the MGE instead of the LGE. Therefore, the limit between the "core" and the positive "shell" around it may represent a bent MGE/LGE boundary. The idea of a bent MGE/LGE boundary agrees with connectivity data in these two portions from the adult avian striatal complex. In birds, the "core" is termed the paleostriatum primitivum (PP) and its projections are pallidal-like: GABAergic and descending into the brainstem, pretectum, and thalamus. The avian "shell" is termed the paleostriatum augmentatum (PA) and its connections are striatal-like in that they receive pallial derivatives and project into the PP (for more on the PP and PA, see Discussion section).

Thus, with a few exceptions that require further clarification, the gene expression patterns analyzed in the chicken forebrain reproduce patterns previously observed in mouse forebrain. In sum, this work represents the first evidence on a molecular level for a conserved mechanism underlying forebrain patterning in chicken and mouse.

Discussion

In vertebrates, the telencephalon is comprised of two main parts demarcated by gene expression patterns: the pallium (cortex) and the subpallium (which include the derivatives of the lateral and medial ganglionic eminences). The pallial region gives rise to the isocortex (termed neocortex in mammals), archicortex, and most likely the paleocortex. In the subpallial region, the lateral ganglionic eminence (LGE) probably gives rise to the striatum; the medial ganglionic eminence (MGE) most likely gives rise to the globus pallidus, the bed nucleus of the stria terminalis, and the amygdala (L. Sussel and J. Rubenstein, unpublished results).

Historically, if an area in the avian brain did not appear to be cortical (as assessed by a laminar organization and connectivity data), researchers assumed it was a striatal derivative. Thus, the nomenclature and assumptions underlying the nomenclature are often vastly different from corresponding structures in the mammalian brain. An area of the striatum present in all primitive vertebrates was termed the archistriatum (AS). Another area common to these species was called the paleostriatum. In birds and reptiles, this area was further divided into the paleostriatum primitivum (PP) and the paleostriatum augmentatum (PA). The PP/PA field was covered by neostriatum in reptiles. In birds, the neostriatum was subdivided into the ectostriatum (ES), nucleus basalis (BAS), and field L (L), an area that is part of the circuitry of bird song. Birds, which evolved from reptiles, show development of a massive dorsal pallial structure called the hyperstriatum (HS).

The telencephalon in avians is predominantly non-laminar; the one exception is an area termed the wulst ("bulge"), which is a laminar visual area. Within the avian telencephalon, the pallium includes the dorsal ventricular ridge (DVR), whose mammalian homologue is much disputed. As supported by data in this thesis, a reasonable conclusion is that the DVR would correspond to the mammalian claustrum, possibly including part of the amygdaloid region. The pallidum would correspond to the basal ventricular ridge (BVR).

The forebrain is extremely complex topographically; its organization is not readily apparent. The prosomeric model (Rubenstein et al., 1994) presents one way to consider the patterning of the forebrain (for details, see Introduction section and references therein). Analyses of gene expression patterns using various molecular markers in mouse and in chicken support the hypothesis that the cephalic neural plate is organized into distinct domains. The extent, however, of segmentation in the forebrain needs to be investigated more closely with additional markers.

As with any working model, there are limitations to the prosomeric model. As more data become available, the model may have to be refined to accommodate this new information. Further, it is important to test whether the prosomeric model will hold true for all species, including lower vertebrates (e.g. the lamprey). Available evidence suggests that the hindbrains of lower vertebrates are segmented; however, it remains to be seen whether the anterior portions of the brain are segmented, as well. In order to be considered segmented, the neuromeric regions must consist of determined neuroepithelium. This is contrasted with being merely regionalized, which is not a developmental mechanism.

This work is complicated by anatomical differences and discrepancies in nomenclature when comparing mouse and chicken brains. The genesis of certain parts is completely different; for example, compare the formation of the wulst in avians with the laminar cortex in mammals. These facts are reflected in a separate nomenclature for chicken and mouse brain areas and structures. Furthermore, the adult structures often look vastly different from the corresponding embryonic areas, termed anlagen or primordia. This contributes to a level of ambiguity when analyzing embryonic areas and structures on morphological data alone.

Although it is a commonly held belief that "higher" vertebrates such as mammals are intellectually superior (and that humans are unique because of their capacity for moral thinking) when compared to "lower" vertebrates, it is not so far-fetched to hypothesize that a similar hierarchy of genes is at work in all vertebrates to form a brain. Based on this study, it appears that the five genes analyzed pattern the avian brain and the murine brain in a similar manner. It must be noted, however, that this does not mean that identical genes are present and performing similar patterning events in each species. Indeed, it is more likely that there is a basic scaffolding of genes which pattern broader areas of the brain, and that the total composition of genes differs as species have evolved. It makes sense, though, that the infinitely efficient and elegant process of evolution may be using similar mechanisms to pattern vertebrate brains, even though the homologous regions in these brains may be performing drastically different tasks.

In sum, this project focuses on the study of gene expression patterns in the forebrain. In order to address this question in a comprehensive manner, further experimental embryological methods should be applied: tissue transplantation studies, correlation of expression patterns with neuronal

projections, etc. Additionally, in order to explore the evolutionary issues more fully, analyses of lower vertebrates should be included.

The analysis of gene expression patterns also can be extended to provide insight into which genes regulate specific developmental processes, and therefore these genes are useful experimental tools for examining the mechanisms that regulate patterning in the CNS.

Emx-1 Introduction

Published previously as Qiu, M-S., Anderson, S., Chen, S., Hevner, R. Kuwana, E., Meneses, J., Pederson, R., Rubenstein, J.L.R. 1996. *Emx-1* mutant mice exhibit abnormal cortical development. *Dev. Biol.* 178: 174-178

After examining the expression pattern of various genes in wild-type mouse and chick embryos, I was interested in a project that was investigating gene expression patterns in mice with gene deletions ("knock-out" mice). In this type of study, a single gene or more is deleted in order to try to examine its role in embryonic forebrain development. These studies often provide clues as to where each gene fits within the genetic hierarchy. For this study, I performed all the *in situ* hybridizations and analyzed the results.

Emx-1 is a homeodomain-containing gene with an expression pattern that is mainly restricted to the cerebral cortex. In order to study its role in forebrain development, a mouse strain lacking a functional *Emx-1* gene was generated.

The first difference that was evident between the wild-type mice and the heterozygotes or homozygotes was in the size and weight of the brain. The brains of the heterozygotes and homozygotes were greatly reduced in size and weight as compared to wild-type brains, generally by half, so that simply by weighing the brains one could guess the genetic status of the mouse. PCR genotyping results confirmed this method of assessing genotype.

To investigate more subtle expression patterns, *in situ* hybridization data were analyzed. The expression pattern of several genes was analyzed: *Tbr-1* (Bulfone et al., 1995), *Nkx-2.1* (Shimamura et al., 1996), *Id-2* (gift from M. Israel), and *Emx-1* and *Otx-1*(Simeone et al., 1992). The amount of

radioactivity incorporated into acid precipitable counts using 1μg of DNA template was as follows:

Emx-1	555,000 cpm
Otx-1	1.8×10^6 cpm
Id-2	983,000 cpm
Tbr-1	1.1×10^6 cpm
Nkx-2.1	683,000 cpm

All probes were used at 1×10^6 cpm.

Upon analysis, there was no discernible phenotype for this knock-out as assessed by *in situ* hybridization for these particular genes. This finding suggests that the EMX-1 protein is not required for maintenance of *Emx-1* expression. The homozygous mice had no obvious morphological or behavioral phenotype. Upon analysis of Nissl-stained sections, however, it was evident that while the cerebral cortex appeared normal, all the homozygous mice lacked most or all or the corpus callosum; these results were confirmed with DiI injections.

It is unclear from this study whether *Emx-1* directly or indirectly regulates corpus callosum development.

Mutation of the *Emx-1* Homeobox Gene Disrupts the Corpus Callosum

Mengsheng Qiu, Stewart Anderson, Sandy Chen, Juanito J. Meneses", Robert Hevner, Ellen Kuwana, Roger A. Pedersen" and John L. R. Rubenstein@

Nina Ireland Laboratory of Developmental Neurobiology, Center for Neurobiology and Psychiatry, Department of Psychiatry and Programs in Neuroscience and Developmental Biology, 401 Parnassus Avenue, University of California at San Francisco, CA, 94143-0984; "Laboratory of Radiobiology and Environmental Health and Department of Obstetrics, Gynecology and Reproductive Sciences, University of California at San Francisco.

Running Title: *Emx-1* mutation disrupts the corpus callosum

@ Address correspondence to:
John L.R. Rubenstein
401 Parnassus Avenue
UCSF
San Francisco, CA, 94143-0984
phone: 415-476-7862
FAX: 415-476-7884
email: jlrr@cgl.ucsf.edu

Abstract

Expression of the *Emx-1* homeobox gene is largely restricted to the developing and mature cerebral cortex. To study its function, two lines of mice were generated using gene targeting methods that have a deletion that includes the N-terminal coding region of *Emx-1*. Mice homozygous for the deletion were viable, fertile and exhibited no obvious behavioral defects. However, 100% of homozygous mice lack most or all of their corpus callosum, the principle fiber tract that connects the left and right cerebral hemispheres. Heterozygotes show partial penetrance for the corpus callosum abnormality. The histology and various molecular properties of the cerebral cortex appear normal in the mutant mice.

Introduction

The cerebral cortex is the seat of higher neurologic functions. An analysis of its development is now possible using genetic methods due to the identification of candidate regulatory genes (Bulfone et al., 1995) and the availability of gene targeting methods. Several homeobox genes related to *Drosophila* gap and segment identity genes have been characterized that are expressed in the developing cerebral cortex, including members of the empty spiracle (*Emx*) and orthodenticle (*Otx*) families (Simeone et al., 1992a,b). Among these genes, only *Emx-1* is primarily expressed in the cerebral cortex, where it is expressed both in proliferating and postmitotic cells (Simeone et al., 1992b; Qiu, Shimamura and Rubenstein, unpublished). Thus, *Emx-1* is a candidate regulator of proliferation, migration and differentiation. To study its role in cortical development, we made a mouse strain lacking a functional *Emx-1* gene.

Materials and Methods

Isolation of *Emx-1* cDNA and Genomic Clones and generation of targeting vector and mutant ES cells

An *Emx-1* cDNA was isolated by screening an E11.5 mouse head library (Qiu unpublished) with a probe homologous to the Drosophila empty spiracle homeobox. The cDNA was sequenced on both strands using oligonucleotide primers and the USB sequenase kit. The cDNA was used to isolate genomic DNA encoding *Emx-1* from 129-strain mice (from Anton Berns, Amsterdam). The targeting construct was made using pBS KS- as the cloning vector. The organization of the targeting vector is shown in Figure 1A (see Qiu et al., 1995 for a description of the components).

The targeting vector was electroporated into JM-1 ES cells, and mutant ES clones were selected and characterized using the methods described in Qiu et al., 1995. Genotyping of ES cells and mice was performed using either Southern blot (Figure 1A) or PCR assays. PCR generates a 273 bp fragment from exon 1; the primers were: 5' ATGGTGGCACCGGCGGGAGT 3' and 5' GGGTTGCAGCGAGGAGGAGC 3'; the conditions were: 1 cycle: 94°C 2 min.; 35 cycles: 94°C 1 min., 63°C 1 min., 72°C 1 min.; 1 cycle: 72°C 6 min.

Northern analysis and *In situ* RNA hybridization

Northern analysis was performed using standard methods (Sambrook et al., 1989). *In situ* hybridization was performed as described in Qiu et al., 1995. The *Otx-1* and Id-2 probes were obtained from Antonio Simeone and Marc Israel, respectively.

Histological analysis

Postnatal animals were sacrificed and perfusion fixed using 4% paraformaldehyde in PBS. The brains were then removed and fixed in 4% paraformaldehyde in PBS for 12 hours and either processed for cryostat or paraffin sectioning. Sections were Nissl-stained to study the general histology of the brain. DiI was used to study the trajectory of the corpus callosum.

Results and Discussion

We generated a mutation in *Emx-1* that resulted in a 2.2 kb deletion between NotI and XhoI sites that removed exon 1 and part of intron 1 (Figure 1A); this removed the N-terminus of the *EMX-1* protein (140 out of 257 amino acids; Qiu and Rubenstein, unpublished). As a result of this mutation, a PGKneo gene cassette was inserted into the deleted region. Two independent ES clones harboring the mutation were identified using Southern analysis, and both of these clones were used to generate mice chimeric of the mutation. Mice chimeric for cell lines #30 and #44 were made, and both transmitted the mutant allele via their germ line. These heterozygous mice were inbred to generate mice homozygous for the mutant allele (Figure 1B). The homozygous mutant mice were viable, fertile and without any obvious morphological or behavioral phenotype. We demonstrated that the homozygous mutant mice lacked *Emx-1* transcripts when probed with a DNA fragment from the deleted region (Figure 1C).

The phenotype of the cerebral cortex was analyzed in the mutant mice of Nissl-stained tissue sections of paraformaldehyde-fixed paraffin-embedded postnatal day 60 brains (Figure 2). We found that 100% of homozygous mutant mice (13 samples analyzed) lacked most or all of the corpus callosum

(a small number of fibers crossed the dorsal midline in the region of the hippocampal commissure; this may be the dorsal commissure of the fornix which is difficult to distinguish from the CC). These findings were confirmed by labeling the subcortical white matter by placing DiI crystals in the cerebral cortex (Figure 2 G,H). None of the wild-type mice (0/15) had an abnormal corpus callosum, whereas 5/15 heterozygotes had this phenotype. We observed abundant white matter collecting adjacent to the commissural plate, and occasional ectopic fibers migrating in the ipsilateral cortex (Probst bundle, see: Ozaki and Wahlsten, 1993). Thus, it appears as though commissural fibers formed, but were not able to cross the commissural plate. At this point it is not clear whether the primary abnormality is in the commissural fibers or in the commissural plate.

The histological appearance of the neocortex, limbic cortex (hippocampus, entorhinal, cingulate, insular), and paleocortex (olfactory bulb and piriform cortex) in the mutant mice were indistinguishable from wild-type littermates. Molecular properties of the mutant cerebral cortex were analyzed by immunohistochemistry and *in situ* RNA hybridization (data not shown). The expression of the glutamate GlnR2-3 receptor in wild-type and mutant adult somatosensory cortex was indistinguishable, showing that the pyramidal projection neurons in layers 2,3 and 5 were present. The expression of *Otx-1*, *Tbr-1* and *Id-2* RNA in the cerebral cortex of wild-type and mutant P6 animals was indistinguishable. The spatial distribution of *Emx-1* expression was unaltered in the mutant, as judged by using a probe from exon 2 (data not shown). This demonstrates that EMX-1 protein is not required for maintenance of *Emx-1* expression.

The CC abnormality can be seen at low penetrance in several inbred mouse strains including 129/J and Balb/c. In these mice, absence of the CC is

found in about 20-30% of adults (Ozaki and Wahlston, 1993). This is of concern because the *Emx-1* mutation was made in ES cells derived from 129/J strain mice. However, the penetrance of the CC phenotype is 100% in *Emx-1-/-*, and we have not detected the CC abnormality in any (0/15) *Emx-1 +/+* litter mates; this strongly suggests that the CC phenotype is due to the *Emx-1* deletion and not due to the genetic background of the mice. Because some of the +/- also show a defective CC (5/15), this phenotype may be *Emx-1* dosage sensitive. The fact that we haven't observed any CC abnormalities in the *Emx-1 +/+* animals may be due to the fact that we have outbred the *Emx-1* +/- mice with C57BL/6 mice, which do not have the CC abnormality.

There are multiple etiologies associated with agenesis or small CC, including at least 70 different human syndromes (Norman et al., 1995). In Balb/c and 129/J mice, Ozaki and Wahlsten (1992, 1993) have provided evidence that an abnormality in the "substrates of axon guidance at the midsagittal plane" are the primary defects that predisposes to the CC defect. Earlier work in Balb/cCF mice reported that failure to form the CC has been associated with a defective transient glial structure (glial sling) that traverses the dorsal midline prior to the formation of the corpus callosum (Silver and Ogawa, 1983). The molecular nature of these defects are not known. As *Emx-1* is expressed in most of the cells in the developing neocortex (Simeone et al., 1992; unpublished data), including those in layers 2 and 3 that are known to contribute processes to the CC, *Emx-1* may regulate the expression of cell surface or other molecules that are required to form the CC. Alternatively, *Emx-1* may regulate morphogenesis of the telencephalon that secondarily affects formation of the CC.

Figure Legends

Figure 1.

Panel A shows a partial map of the *Emx-1* genomic organization; the location of exons 1 and 2 (boxes), and the position of BamH1 (B), EcoR1 (E), Not1 (N) and Xho1 (X) sites are indicated. The positions of probes (P1 and P2) used for southern analysis are shown. In the middle is shown the *Emx-1* targeting vector, indicating the 2.2 kb deletion that includes exon 1 (between Xho1 and Not1), and the insertion of the PGKneo cassette, oriented in parallel to the direction of *Emx-1* transcription. The bottom tier shows the structure of the mutated *Emx-1* locus.

Panel B shows a Southern analysis of F2 progeny using Probe 1 (P1) and an EcoR1 digest; the wild-type fragment is 10.5 kb, the mutant fragment is 6 kb.

Panel C is a Northern analysis of wild-type, heterozygote and homozygote mutant E14.5 embryos, using probe 2 (P2).

Figure 2.

Nissl-stained cryostat coronal sections of wild-type (A,C,E) and homozygote mutant (B,D,F) 10 week old litter mates. The mutant animals lack most of the corpus callosum (CC); a residual CC can be seen in panel F, overlying the hippocampal commissure (hcc). A bundle of fibres (Probst bundle, pb), that may include fibres that would otherwise contribute to the CC, are seen in panel B. DiI-labeled wild-type (G) and homozygous mutant (H) coronal sections, just rostral to the locations shown in E and F, showing that some fibres cross the midline in the mutant. The DiI crystal was applied to the parietal cortex. The dotted line marks the dorsal midline of the cerebral

cortex. Other abbreviations: ac: anterior commissure; cx: neocortex; sp: septum; st: striatum. The magnification bars in panels D and H are 500 microns.

Acknowledgements

This work was supported by grants to JLRR (March of Dimes, NARSAD, the John Merck Fund, Pfizer Pharmaceuticals, and NIMH RO1 MH49428-01 and K02 MH01046-01), MSQ (NIH FS NS09874), SA (NARSAD, VA), RAP (NICHD P0-1, HD26732 and US DOE/OHER Contract No. DE-ACO3-76-SF01012). We thank D. Walhsten for fruitful discussions.

References

Bulfone, A., Smiga, S.M., Shimamura, K., Puelles, L., Peterson, A. and Rubenstein, J.L.R. (1995). T-Brain (Tbr-1): A homologue of Brachyury whose expression defines molecularly distinct domains within the cerebral cortex. *Neuron*, **15**, 63-78.

Ozaki, H.S. and Wahlsten, D. (1992). Prenatal formation of the normal mouse corpus callosum: a quantiative study with carbocyanine dyes. *J. Comp. Neurol.* **323**, 81-90.

Ozaki, H.S. and Wahlsten, D. (1993). Cortical axon trajectories and growth cone morphologies in fetuses of acallosal mouse strain. *J. Comp. Neurol.* **336**, 595-604.

Norman, M.C., McGillivray, B.C., Kalousek, D.K., Hill, A., and Poskitt, K.J. (1995). Congenital Malformations of the Brain. Oxford Press.

Qiu, M., Bulfone, A., Martinez, S., Meneses, J.J., Shimamura, K., Pedersen, R.A. and Rubenstein, J.L.R. (1995). Role of *Dlx-2* in Head Development and Evolution: Null Mutation of *Dlx-2* Results in Abnormal Morphogenesis of Proximal First and Second Branchial Arch Derivatives and Abnormal Differentiation in the Forebrain. *Genes and Development*, **9**, 2523-2538.

Silver, J. and Ogawa, M.Y. (1983). Postnatally induced formation of the corpus callosum in acallosal mice on glia-coated cellulose bridges. *Science* **22**, 1067-1069

Simeone, A., Acampora, D., Gulisano, M., Stornaiuolo, A., and Boncinelli, E. (1992a). Nested expression domains of four homeobox genes in developing rostral brain. *Nature* **358**, 687-690.

Simeone, A., Gulisano, M., Acampora, D., Stornaiuolo, A., Rambaldi, M., and Boncinelli, E. (1992b). Two vertebrate homeobox genes related to the *Drosophila empty spiracles* gene are expressed in the embryonic cerebral cortex. *EMBO J.* ***11***, 2541-2550.

A. *Emx-1* genomic organization and targeting strategy

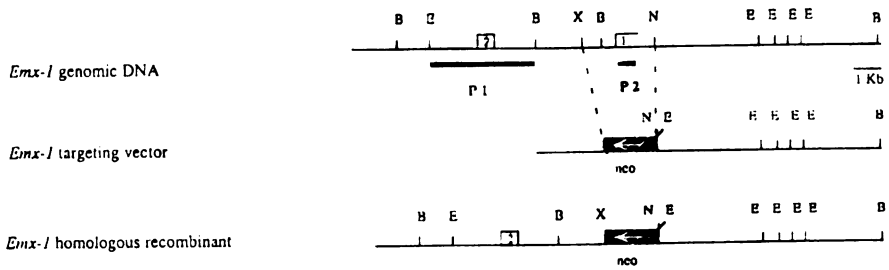

B. Southern analysis of the *Emx-1* F2 Progeny

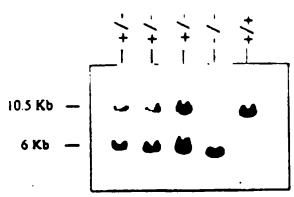

Probe 1

C. Absence of *Emx-1* expression in the E14.5 homozygous embryos

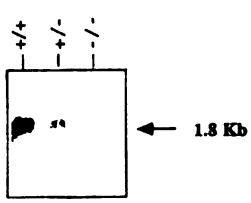

Probe 2

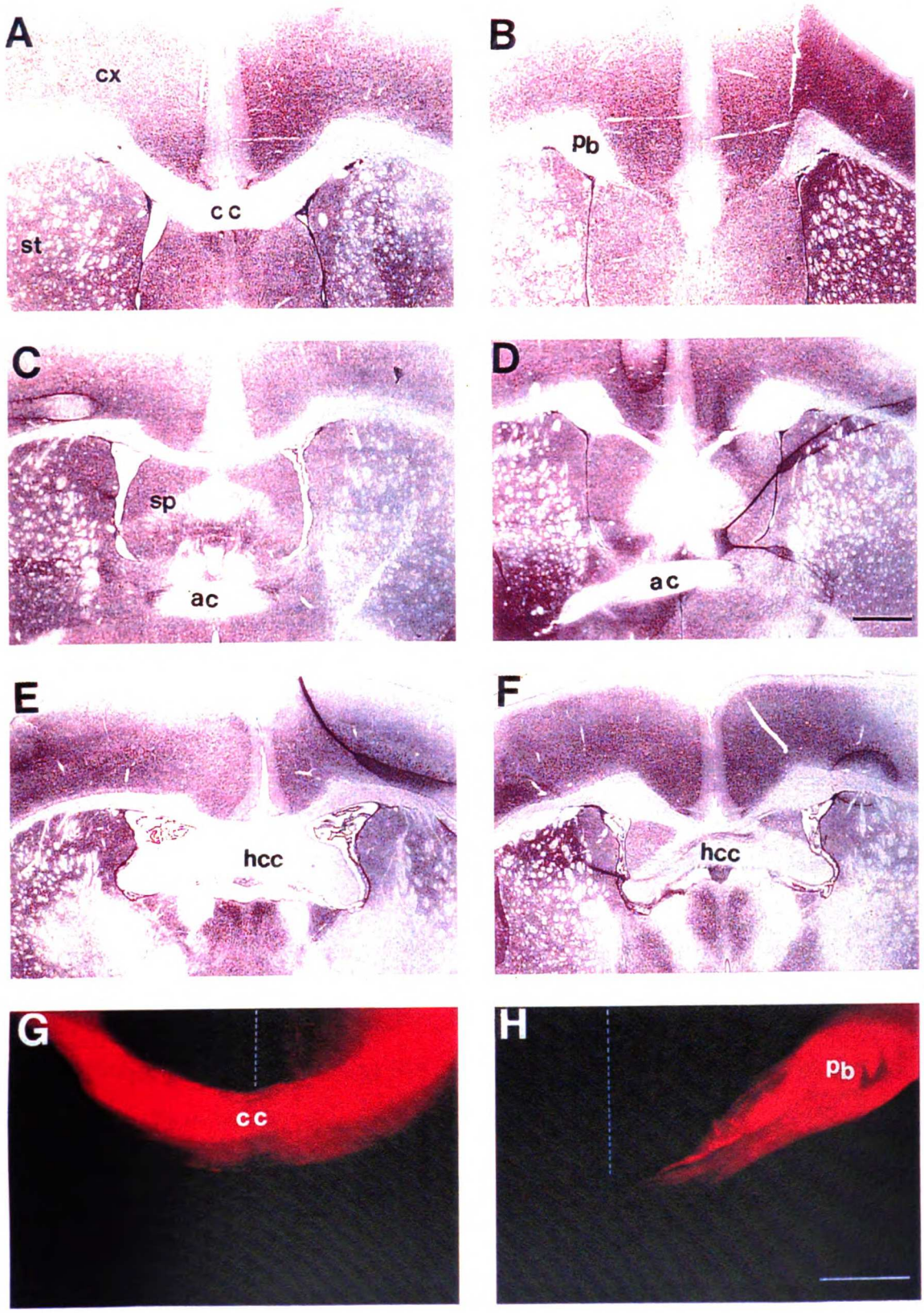
A
cx
cc
st
B
pb
C
sp
ac
D
ac
E
hcc
F
hcc
G
cc
H
pb

References

Alvarez-Bollado, G., Rosenfeld, M.G., Swanson, L.W. 1995. Model of forebrain regionalization based on spatiotemporal patterns of POU-III homeobox gene expression, birthdates, and morphological features.
J. Comp. Neurol. 355: 237-295

Ang, S.L., Jin, O., Rhin, M., Daigle, N., Stevenson, L., Rossant, J. 1996. A targeted mouse *Otx2* mutation leads to severe defects in gastrulation and formation of axial mesoderm and to deletion of rostral brain. *Development* 122 (1): 243-252

Baumgartner, S., Bopp, D., Burri, M., Noll, M. 1987. Structure of two genes at the *gooseberry* locus related to the *paired* gene and their spatial expresssion during *Drosophila* embryogenesis. *Genes Dev.* 1: 1247-67

Boncinelli, E., Gulisano, M., Spada, F., Broccoli, V. 1995. *Emx* and *Otx* gene expression in the developing mouse brain. *Ciba Foundation Symposium* 193: 100-126

Bopp, D., Burri, M., Baumgartner, S., Frigerio, G., Noll, M. 1986. Conservation of a large protein domain in the segmentation gene *paired* and in the functionally related genes of *Drosophila. Cell* 47: 1033-40

Bulfone A., Puelles, L., Porteus, M.H., Frohman, M.A., Martin, G.R., Rubenstein, J.L.R. 1993a. Spatially restricted expression of *Dlx-1, Dlx-2* (*Tes-1*), *Gbx-2*, and *Wnt-3* in the embryonic day 12.5 mouse forebrain defines

potential transverse and longitudinal segmental boundaries. *J. Neuroscience* 13: 3155-3172

Bulfone, A., Kim, H-J., Puelles, L., Porteus, M.H., Grippo, J.F., Rubenstein, J.L.R. 1993b. The mouse *Dlx-2* (*Tes-1*) gene is expressed in spatially restricted domains of the forebrain, face, and limbs in midgestation mouse embryos. *Mechanisms of Development* 40: 129-140

Bulfone, A., Smiga, S., Shimamura, K., Puelles, L., Peterson, A., Rubenstein, J.L.R. 1995. T-Brain (*Tbr-1*): A homologue of *Brachyury* whose expression defines molecularly distinct domains within the cerebral cortex. *Neuron* 15: 63-78

Chalepakis, G., Stoykova, A., Wijnholds, J., Tremblay, P., Gruss, P. 1993. *Pax*: gene regulators in the developing nervous system. *J. Neurobiol.* 24: 1367-1384

Couly, G. and Le Douarin, N.M. 1988. The fate map of the cephalic neural primordium at the presomitic to the 3-somite stage in the avian embryo. *Development Suppl.* 103: 101-113

Dressler, G.R., Deutsch, U., Balling, R., Simon, D., Guenet, J-L., Gruss, P. 1988. Murine genes with homology to *Drosophila* segmentation genes. *Development Suppl.* 104: 181-86

Gall, J.G., Cohen, E.H., Polan, M.L. 1971. Repetitive DNA sequences in *Drosophila*. *Chromosoma* 33 (3): 319-44

Guthrie, S. 1995. The status of the neural segment. *TINS* 18 (2): 74-79

Karten, H. 1991. Homology and evolutionary origins of the 'neocortex'. *Brian Behav. Evol.* 38:264-272

Kaufman, M.H. 1992. *The Atlas of Mouse Development.* Academic Press Limited, London

Keynes, R. and Lumsden, A. 1990. Segmentation and the origin of regional diversity in the vertebrate central nervous system. *Neuron* 2: 1-9

Keynes, R. and Krumlauf, R. 1994. *Hox* genes and regionalization of the nervous system. *Ann. Rev. Neurosci.* 17: 109-132

Kim, Y. and Nirenberg, M. 1989. *Drosophila* NK-homeobox genes. *PNAS* 86 (20): 7716-7720

Krubitzer, L. 1995. The organization of neocortex in mammals: are species differences really so different? *Trends Neurosci.* 18: 408-417

Krumlauf, R., Marshall, H., Studer, M., Nonchev, S., Sham, M.H., Lumsden, A. 1993. *Hox* homeobox genes and regionalisation of the nervous system. *J. Neurobiol.* 24 (10): 1328-40

Krumlauf, R. 1994. *Hox* genes in vertebrate development. *Cell* 78: 191-201

Kuhlenbeck, H. 1973. *The Central Nervous System of Vertebrates.* Vol. 3, Part II. Berlin: S. Karger, A.G.

Lazzaro, D., Price, M., De Felice, M., Di Lauro, R. 1991. The thyroid transcription factor TTF-1 is expressed at the onset of thyroid and lung morphogenesis and in restricted regions in the fetal brain. *Development* 113: 1093-1104

McGinnis, W. and Krumlauf, R. 1992. Homeobox genes and axial patterning. *Cell* 68: 283-302

McGuinness, T., Porteus, M.H., Smiga, S., Bulfone, A., Kingsley, C., Qiu, M., Liu, J.K., Long, J.E., Czernik, A., Xu, D., Rubenstein, J.L.R. 1996. Sequence, organization and transcription of the *Dlx-1* and *Dlx-2* locus. *Genomics* 35: 473-85

Murre, C., McCaw, P.S., Vaessin, H., Caudy, M., Jan, L.Y., Jan, Y.N., Cabrera, C.V., Buskin, J.N., Hauschka, S.D., Lassar, A.B., et al. 1989. Interactions between heterologous helix-loop-helix proteins generate complexes that bind specifically to a common DNA sequence. *Cell* 58 (3): 537-44

Northcutt, G.R. and Kaas, J.H. 1995. The emergence and evolution of mammalian neocortex. *Trends Neurosci.* 18: 373-379

Porteus, M.H., Bulfone, A., Ciaranello, R.D., Rubenstein J.L.R. 1991. Isolation and characterization of a novel cDNA clone encoding a homeodomain that is developmentally regulated in the ventral forebrain. *Neuron* 7: 221-229

Porteus, M.H., Brice, J.E.A., Usdin, T.B., Ciaranello, R.D., Rubenstein, J.L.R. 1992. Isolation and characterization of a library of cDNA clones that are preferentially expressed in the embryonic telencephalon. *Molecular Brain Research* 12: 7-22

Porteus, M.H., Bulfone, A., Lui, J-K., Puelles, L., Lo, L-C., Rubenstein, J.L.R. 1994. *Dlx-2, Mash-1* and *Map-2* expression and bromodeoxyuridine incorporation define molecularly distinct cell populations in the embryonic mouse forebrain. *J. Neuroscience* 14: 6370-6383

Povinelli, D.J. and Preuss, T.M. 1995. Theory of mind: evolutionary history of a cognitive specialization. *Trends Neurosci.* 18: 418-424

Price, M., Lazzaro, D., Pohl, T., Mattei, M-G., Ruther, U., Olivo, J-C., Duboule, D., Di Lauro, R. 1992. Regional expression of the homeobox gene *Nkx-2.2* in the developing mammalian forebrain. *Neuron* 8: 241-55

Price, M. 1993. Members of the *Dlx-* and *Nkx2*-gene families are regionally expressed in the developing forebrain. *J. Neurobiol.* 24 (10): 1385-1399

Puelles, L., Amat, J.A., Martinez-de-la-Torre, M. 1987. Segment-related, mosaic neurogenetic pattern in the forebrain and mesencephalon of early chick embryos: I. Topography of AChE-positive neuroblasts up to stage HH18. *J. Comparative Neurology* 226 (2): 247-268

Puelles, L. and Rubenstein, J.L.R. 1993. Expression patterns of homeobox and other putative regulatory genes in the embryonic mouse forebrain suggest a neuromeric organization. *Trends Neurosci.* 16: 472-479

Puelles, L. 1995. A segmental morphological paradigm for understanding vertebrate forebrains. *Brain Behav. Evol.* 46: 319-337

Qiu, M-S., Bulfone, A., Martinez, S., Meneses, J.J., Shimamura, K., Pedersen, R.A., Rubenstein, J.L.R. 1995a. Role of *Dlx-2* in head development and evolution: Null mutation of *Dlx-2* results in abnormal morphogenesis of proximal first and second branchial arch derivatives and abnormal differentiation in the forebrain. *Genes and Development* 9: 2523-2538

Qiu, M-S., Anderson, S., Chen, S., Hevner, R., Kuwana, E., Meneses, J., Pedersen, R., Rubenstein, J.L.R. 1996. *Emx-1* mutant mice exhibit abnormal cortical development. *Developmental Biology* 178: 174-78

Rubenstein, J.L.R., Martinez, S., Shimamura, K., Puelles, L. 1994. The embryonic vertebrate forebrain: the Prosomeric model. *Science* 266: 578-580

Ruiz i Altaba, A. 1994. Pattern formation in the vertebrate neural plate. *TINS* 17: 233-243

Shimamura, K., Hartigan, D.J., Martinez, S., Puelles, L., Rubenstein, J.L.R. 1995. Longitudinal organization of the anterior neural plate and neural tube. *Development* 121: 3923-3933

Shimamura, K., Martinez, S., Puelles, L., Rubenstein, J.L.R. 1996. Patterns of gene expression in the neural plate and neural tube subdivide the embryonic forebrain into transverse and longitudinal domains. *Developmental Neuroscience*, in press

Simeone, A., Gulisano, M., Acampora, D., Stornaiuolo, A., Rambaldi, M., Boncinelli, E. 1992a. Two vertebrate homeobox genes related to the *Drosophila empty spiracles* gene are expressed in the embryonic cerebral cortex. *EMBO J.* 11: 2541-2550

Simeone, A., Acampora, D., Gulisano, M., Stornaiuolo, A., Boncinelli, E. 1992b. Nested expression domains of four homeobox genes in developing rostral brain. *Nature* 358: 687-690

Stoykova, A. and Gruss, P. 1994. Roles of *Pax*-genes in developing and adult brain as suggested by expression patterns. *J. Neurosci.* 14: 1395-1412

Theiler, K. 1989. *The House Mouse: Atlas of Embryonic Development.* Springer-Verlag, New York

Tole, S. and Patterson, P.H. 1995. Regionalization of the developing forebrain: a comparison of *FORSE-1*, *Dlx-2* and *BF-1*. *J. Neurosci.* 15 (2): 970-80

Walther, C. and Gruss, P. 1991. *Pax-6*, a murine paired box gene, is expressed in the developing CNS. *Development* 113: 1435-1449

Zoeller, R.T., Seeburg, P.H., Young, W.S. III. 1988. *In situ* hybridization for messenger ribonucleic acid (mRNA) encoding gonadotropin-releasing hormone (GnRH): effect of estrogen on cellular levels of GnRH mRNA in female rat brain. *Endocrinology* 122 (6): 2570-2577

Appendix I

Preparation of Tissue

PARAFORMALDEHYDE (PFA) FIXATION

Make fresh on day of use.

Use diethyl pyrocarbonate- (DEPC-) treated solutions and water.

1. Place isolated tissue in 4% PFA in 1x phosphate-buffered saline (PBS) with 4% sucrose:

   5 ml 20x PBS, Ca^{++} Mg^{++}Free

   4 g PFA

   100 ml total in water

   Heat at 65° Celsius until dissolved.

   Add 4 g sucrose, dissolve, filter and store at 4° Celsius.

2. Fix tissues according to size and permeability.

   For example:

mouse age	time of fixation
E8.5	1 hour
E9.5	3 hours
E10.5	5 hours
E11.5	overnight

chick age	time of fixation
E5.0	8 hours
E8.5	overnight
E10.5	overnight
E14.5	overnight

SUCROSE INFUSION

Use DEPC-treated solutions and water.

1. Put tissue in graded sucrose solutions until tissue is equilibrated ("sinks").

   10% sucrose in 1x PBS

   20% sucrose in 1x PBS

   30% sucrose in 1x PBS

OCT EQUILIBRATION

1. Put tissue in solution of 50% OCT (Tissue Tek Embedding Medium) and 50% of the 30% sucrose solution.
2. Rock gently at 4° Celsius for 1 hour.
3. Transfer tissue to 100% OCT.
4. Rock gently at 4° Celsius for 1 hour.
5. Rinse twice in 100% OCT to remove any sucrose from outside of tissue.

EMBEDDING TISSUE

1. Transfer tissue to embedding mold filled with OCT.
2. Position brain as desired.
3. Freeze sample by placing embedding mold in 2-methylbutane cooled to the temperature of dry ice, making sure that the surface is flat.
4. Once frozen, store at -80° Celsius.

Appendix II

Preparation of Template DNA for ^{35}S Riboprobe

LINEARIZATION

1. Add

   10 µg CsCl-pure template DNA

   5 µl appropriate restriction enzyme

   10 µl appropriate enzyme buffer

   100 µl total in water

   Place at 37° Celsius for 3 hours.

2. Run DNA on 1% agarose gel.

   50 ml 1x Tris-acetate buffer (TAE)

   1 g agarose

   1 µl ethidium bromide (EtBr)

   Load 0.5 µl DNA with 1 µl 6x loading dye and 3.5 µl water.

   Load 5 µl 1 kb ladder.

3. Run gel 45 minutes at 65 volts, confirm DNA is linearized.

PURIFICATION

1. Add 50 µl/ml proteinase K at 10 mg/ml to template DNA.

   Incubate 30 minutes at 37° Celsius.

2. Add DEPC-treated water to volume of 200 µl.

3. Extract twice with 200 µl 1:1 phenol-chloroform, chloroform extract once.

4. Add 20 µl (=1/10 volume) 3 M NaOAc, pH 5.2

   Add 440 µl 100% ethanol (EtOH), vortex.

5. Place at -80° Celsius overnight or at -20° Celsius for 30 minutes.
6. Spin 20 minutes.
7. Aspirate pellet and wash with 70% EtOH.
8. Spin 10 minutes.
9. Aspirate pellet, wash with 100% EtOH.
10. Air dry completely.
11. Resuspend in 10 µl DEPC-water to a final concentration of 1 µg/ul.

Appendix III

Synthesis of ^{35}S Riboprobe

Use an *in vitro* transcription kit (Stratagene #200340).

1. Add in order the following:

   2 µl DEPC-treated water

   5 µl 5x transcription buffer

   2 µl DNA template

   1 µl 0.75 M dithiothreitol (DTT)

   1 µl 10 mM rATP

   1 µl 10 mM rCTP

   1 µl 10 mM rGTP

   1 µl RNase block, 40 units/µl

   8-10 µl ^{35}S UTP

   1 µl appropriate RNA polymerase

2. Place at 37° Celsius for 1 hour.
3. Add 0.5 µl appropriate RNA polymerase.
4. Place at 37° Celsius for 30 minutes.
5. Add 2 µl tRNA, 10 mg/ml and

   1 µl RNase-free DNase I, 10 units/µl (Stratagene #600031).

6. Place at 37° Celsius for 10 minutes.
7. Add 65 µl water (DEPC-treated)

   1 µl 0.75 M DTT

   3 µl tRNA

   10 µl 3 M NaOAc, pH 5.2

8. Vortex, extract with 100 µl 1:1 phenol-chloroform.
9. Repeat phenol-chloroform extraction.

10. Add 100 µl (=1 volume) 4M NH_4OAc.

    250 µl 100% EtOH

11. Place at -20° Celsius overnight or -80° Celsius for 30 minutes.

12. Spin 20 minutes, aspirate pellet, wash with 500 µl 70% EtOH.

13. Spin 10 minutes, aspirate pellet, wash with 500 µl 100% EtOH.

14. Dry pellet completely.

15. Resuspend in 50 µl 10 mM DTT.

16. Count 1 µl probe in 1-2 ml scintillation cocktail.

Appendix IV

Alkaline Hydrolysis of ^{35}S Riboprobe

This procedure is recommended for probes exceeding 1.7 kb. It will hydrolyze the probe to 300 bp fragments. The following formula is the basis for the protocol:

$T\ (min) = l_o - l_f / k * l_o * l_f$	where	l_o= original length of probe (kb) l_f= final length (kb) k= 0.11 cuts/kb/minute

1. To 50 µl of probe, add a 1:1 solution of
   1 M $NaHCO_3$
   1 M Na_2CO_3
2. Incubate at 60° Celsius for required time.

original length (kb)	reaction time (min)
0.75	18
1.0	21
2.0	25
2.8	27

3. Add
   3 µl 10% acetic acid
   4 µl tRNA, 5 mg/ml
   100 µl 4 M NH_4OAc
   Vortex, add 400 µl 100% EtOH.
4. Incubate at -80° Celsius for 30 minutes or overnight at -20° Celsius.
5. Spin 20 minutes, aspirate pellet, wash with 80% EtOH.
6. Resuspend in 50 µl of 10 mM DTT.
7. Count 1 µl in 1-2 ml scintillation cocktail.

Appendix V

In Situ Hybridization Protocol

PREHYBRIDIZATION

Use DEPC-treated solutions and water.

1. Allow slides to air dry at least 20 minutes and up to 2 hours.
2. Place slides in 4% PFA in 1x PBS at room temperature for 20 minutes.
3. Wash in 3x PBS for 4 minutes.
4. Wash twice in 1x PBS for 4 minutes each.
5. Rinse in DEPC-treated water.
6. Dehydrate through graded EtOH: 50, 80, and 95% for 2 minutes each.
7. Air dry.

PROTEINASE K TREATMENT

Use DEPC-treated solutions and water.

1. Incubate slides in 1µg/ml proteinase K at room temperature for 20 minutes: 1 µg/ml proteinase K in 100 mM Tris-HCl at pH 8 and 50 mM disodium ethylene diamine tetraacetate (EDTA).
2. Post-fix for 5 minutes in 4% PFA in 1x PBS (DEPC-treated).

ACETYLATION

Use DEPC-treated solutions and water.

1. Put slides in 0.1 M triethanolamine (TEA) stirring on stir plate: 2.6 ml of 7.5 M TEA in 200 ml DEPC-treated water.
2. Add 500 µl acetic anhydride, stir 5 minutes.
3. Let sit 5 minutes.

4. Dehydrate through graded EtOH as above.
5. Air dry.

HYBRIDIZATION

1. Heat $2x10^6$ counts per minute (cpm) labeled riboprobe per slide in 100 µl hybridization buffer (see Appendix IX for details) per slide at 65° Celsius for 5 minutes.
2. Add 100 µl to each slide.
3. Cover with parafilm coverslip, dimensions 2x2 cm or 2x2.5 cm.
4. Incubate in humidified chamber at 52° Celsius for 18 hours.

POST-HYBRIDIZATION WASHES

DEPC-treated solutions and water not necessary.

1. Wash slides in 2x sodium chloride-sodium citrate (SSC) with 10 mM ß-mercaptoethanol (ß-ME) for 30 minutes at room temperature after removing coverslips.
2. Wash in 2x SSC with 1 mM EDTA containing 20 µg/ml RNase A and 1 unit/ml RNase T1 for 40 minutes at room temperature.
3. Wash 2x in 50% formamide with 2x SSC, 1 mM EDTA, and 10 mM ß-ME at 55° Celsius for 30 minutes each.
4. Wash in 0.2x SSC for 2 minutes.
5. Dehydrate through graded EtOH as above.
6. Air dry.
7. Tape slides to an old piece of film or cardboard film insert, expose overnight on X-ray film to check signal.

Appendix VI

Autoradiography

DIPPING SLIDES

Make emulsion mix in darkroom on day of use.

DEPC-treated solutions and water not necessary.

1. Melt 15 ml of NTB2 emulsion in 50 ml Falcon tube in 42° Celsius water bath in darkroom. Allow 30-40 minutes.
2. Dilute 1:1 with prewarmed distilled water with 1% glycerol added. Leave at 40° Celsius until emulsion is dissolved completely.
3. Transfer solution to a plastic cytology slide mailer, pouring onto the side of the mailer held at an angle so as to avoid bubble formation. Check solution is free of bubbles by dipping several slides until no bubbles are evident.
4. Dip slides twice slowly and gently, then wipe back of slide clear of emulsion, set on flat surface to air dry for approximately 2 hours.
5. Put completely dry slides into a light-tight slide box, add desiccant, seal with tape and wrap in foil to protect from light. Store at 4° Celsius for 10-14 days.
6. Make sure that no ^{32}P or organic solvents are stored with exposed slides, as exposure to either will increase background levels.

DEVELOPING SLIDES

Steps 1-6 must be performed in the darkroom.

1. Remove box(es) from 4° Celsius storage and let warm to room temperature. Slides and developing solutions should be near the same temperature or the emulsion will wrinkle.
2. Make developer and fix solutions ahead of time, cool to approximately 16° Celsius. Pour solutions into glass slide racks and chambers (ones used for histological staining).
3. In darkroom, put slides in Kodak D-19 developer solution diluted 1:1 with distilled water for 5 minutes.
4. Transfer to chilled distilled water for 30 seconds.
5. Place slides in Kodak fixer for 8 minutes.
6. Rinse slides in gently running tap water for 20 minutes.
7. Counterstain sections in 0.1% toluidine blue containing 10 mM sodium acetate at pH 4.7 for 10 minutes.
8. Rinse in tap water until water runs clear.
9. Dehydrate through graded ethanols: 50, 80, 95, and 100%.
10. Mount coverslips using Permount histological mounting medium (Fisher).

SOLUTIONS

1. Fixer

   Add 89.5 g of fixer to 500 ml total water.

   Stir until dissolved, filter and store at 4° Celsius.

2. Developer

   Add 39.15 g developer to 250 ml total water.

   Stir at 55° Celsius until dissolved, dilute 1:1 with water.

   Filter and store at 4° Celsius.

Appendix VII

In Situ Hybridization Solutions

1. 4% PFA in 1x PBS

   16 g PFA

   40 ml 10x PBS, Ca^{++} Mg^{++} Free

   400 ml total in water

   Place at 60° Celsius until dissolved, filter.

2. 3x PBS

   60 ml 10x PBS

   200 ml total in water (depc-treated)

3. Proteinase K

   20 ml 1 M Tris

   20 ml 0.5 M EDTA, pH 8.0

   200 ml total in water (DEPC-treated)

   20 µl Proteinase K, 10 mg/ml

4. TEA

   2.6 ml 7.5 M TEA

   200 ml total in water (DEPC-treated)

   Stir on stir plate, once slides are in, add 500 µl acetic anhydride.

APPENDIX VIII

Post-hybridization Solutions

DEPC-treated solutions and water not necessary.

1. 2x SSC, 10 mM ß-ME

   50 ml 20x SSC

   390 µl ß-ME

   500 ml total in distilled water

2. 2x SSC, 1 mM EDTA, 20 µg/ml RNase A

   40 ml 20x SSC

   800 µl 0.5 M EDTA, pH 8.0

   400 ml total in distilled water

   Split into two containers, to each container add

   1µl RNase T1 and

   400 µl RNase A (heated at 95° Celsius for 10 minutes).

3. 50% formamide, 2x SSC, 1 mM EDTA, 10 mM ß-ME

   80 ml 20x SSC

   1.6 ml 0.5M EDTA, pH 8.0

   625 µl ß-ME

   200 ml formamide

   400 ml total in distilled water

Appendix IX

Hybridization Buffer

1. Add the following in order:

Final Concentration	Amount to Add
50% formamide	25 ml low grade formamide
5x SSC	12.5 ml DEPC-20x SSC
2x Denhardts	2 ml 50x Denhardts
10% dextran sulfate	5 g dextran sulfate
500 µg/ml ssDNA	2 ml ssDNA, 12 mg/ml
250 µg/ml yeast tRNA	470 µl yeast tRNA, 25 mg/ml
10 mM ß-ME	35 µl ß-ME

2. Add DEPC-treated water to 50 ml total.
3. Aliquot and store at -80° Celsius.

Appendix X

Synopsis of Chick Development

taken from Hamburger and Hamilton staging

Stage(s)	Time Elapsed	Description of Developmental Events
2-6	up to 24 hours	Hensen's node, notochord visible
		1 somite forms
6-12	up to 48 hours	3 brain vesicles apparent
		5 distinct neuromeres in hindbrain seen
		optic vesicles and stalk visible
		approximately 16 somites forms
12-17	up to 72 hours	forebrain and hindbrain at right angle
		Rathke's pouch visible
		nasal pits forms
		approximately 32 somites forms
18-22	3 days	leg and wing buds starting to form
		maxillary and mandibulary processes form
		eye pigmentation visible
		approximately 43 somites forms
23-25	4 days	limbs buds appear longer than wide
		elbow and knee joints visible
26-28	5 days	toe development visible
		branchial arch development continues
		beak visible
29-30	6 days	webs between toes apparent
		auditory meatus forms
		beak more prominent

		3 segments within leg and wing visible
		egg tooth evident
31-33	7 days	feather germs begin developing
34-35	8 days	nictitating membrane of eye halfway between eyelid and scleral papillae
35	9 days	phalanges in toe distinct
		feather germs more noticeable
		nictitating membrane to outer scleral papillae
36	10 days	primordia of claws and comb visible
		beak length approximately 2.5 mm
37	11 days	pads on plantar surface of foot seen
		beak length of approximately 3.0 mm
38	12 days	primordia of scales on legs seen
		reduced opening between lids of eye evident
		beak length of approximately 3.1 mm
39	13 days	increase in length of feather germs seen
		space between lids reduced to crescent
		beak length of approximately 3.5 mm
40	14 days	beak length of approximately 4.0 mm
41	15 days	beak length of approximately 4.5 mm
42	16 days	beak length of approximately 4.8 mm
43	17days	beak length of approximately 5.0 mm
44	18 days	beak length of approximately 5.7 mm
45	19-20 days	beak appears shiny and blunted at tip
		yolk sac half enclosed in body cavity
46	20-21 days	chick hatches

Appendix XI

Synopsis of Mouse Development

taken from The Atlas of Mouse Development by M.H. Kaufman, 1992

staging based on K.Theiler, 1989

Stage(s)	Time Elapsed	Description of Developmental Events
St 7	5.5 days	embryo implantation
St 9	6.5 days	mesoderm formation
St 10	7 days	primitive groove evident
St 12	8 days	appearance of first (1-7) somites
		neural fold closure, neural plate evident
St 13	8.5 days	8-12 somites evident
		"turning" stage, optic sulcus visible
		second branchial arch evident
St 14	9 days	13-20 somites visible
		rostral neuropore, optic vesicle formation
St 15	9.5 days	21-29 somites visible
		third ventricle, telencephalic vesicles formed
		caudal neuropore, optic pit formation
		forelimb buds evident
St 16	10 days	30-34 somites evident
		caudal neuropore closure
		hindlimb buds evident
		lens placode, otic vesicle, olfactory pit seen
St 17	10.5	35-39 somites visible
		lens vesicle formation

St 18	11 days	40-44 somites evident
		deep nasal pit, lens vesicle visible
St 19	11.5 days	43-48 somites apparent
		cervical somites indistinct
		lens vesicle separates from surface ectoderm
St 20	12 days	48-52 somites seen
		handplate differentiation
		eye pigmentation visible
St 21	13 days	52-55 somites evident
		vibrissae precursors formation
		digit formation in hand and footplates
		choroid plexus distinguishable
St 22	14 days	60 somites visible
St 23	15 days	60-65 somites evident
		development of handplate digits
		olfactory lobes distinguishable
St 24	16 days	eyelid closure
		appearance of hair follicles
St 25	17 days	formation of skin wrinkles
		vibrissae on upper lip area apparent
		pads on hand and foot surfaces prominent
St 26	18 days	embryo resembles postnatal mouse

Figure 1.

Comparison of *Tbr-1, Pax-6, Dlx-2,* and *Emx-1* expression patterns using *in situ* RNA hybridization to mouse E13.5 coronal sections. Sections are ordered rostral (a, b, c, d) to caudal (m, n, o, p).

1st column: a, b, c, d represent section numbers 20, 19, 17, 18, respectively.

2nd column: e, f, g, h represent section numbers 49, 48, 46, 47, respectively.

3rd column: i, j, k, l represent section numbers 59, 58, 56, 57, respectively.

4th column: m, n, o, p represent section numbers 69, 68, 66, 67, respectively.

Sections a, e, i, m were analyzed for *Tbr-1* expression; sections b, f, j, n for *Pax-6*; sections c, g, k, o for *Dlx-2*; sections d, h, l, p for *Emx-1.*

^{35}S probes were used for all sections. Abbreviations are as defined in the Glossary. All sections were photographed using dark-field microscopy. All sections were from a single mouse embryo.

Figure 1: Mouse E13.5 horizontal sections

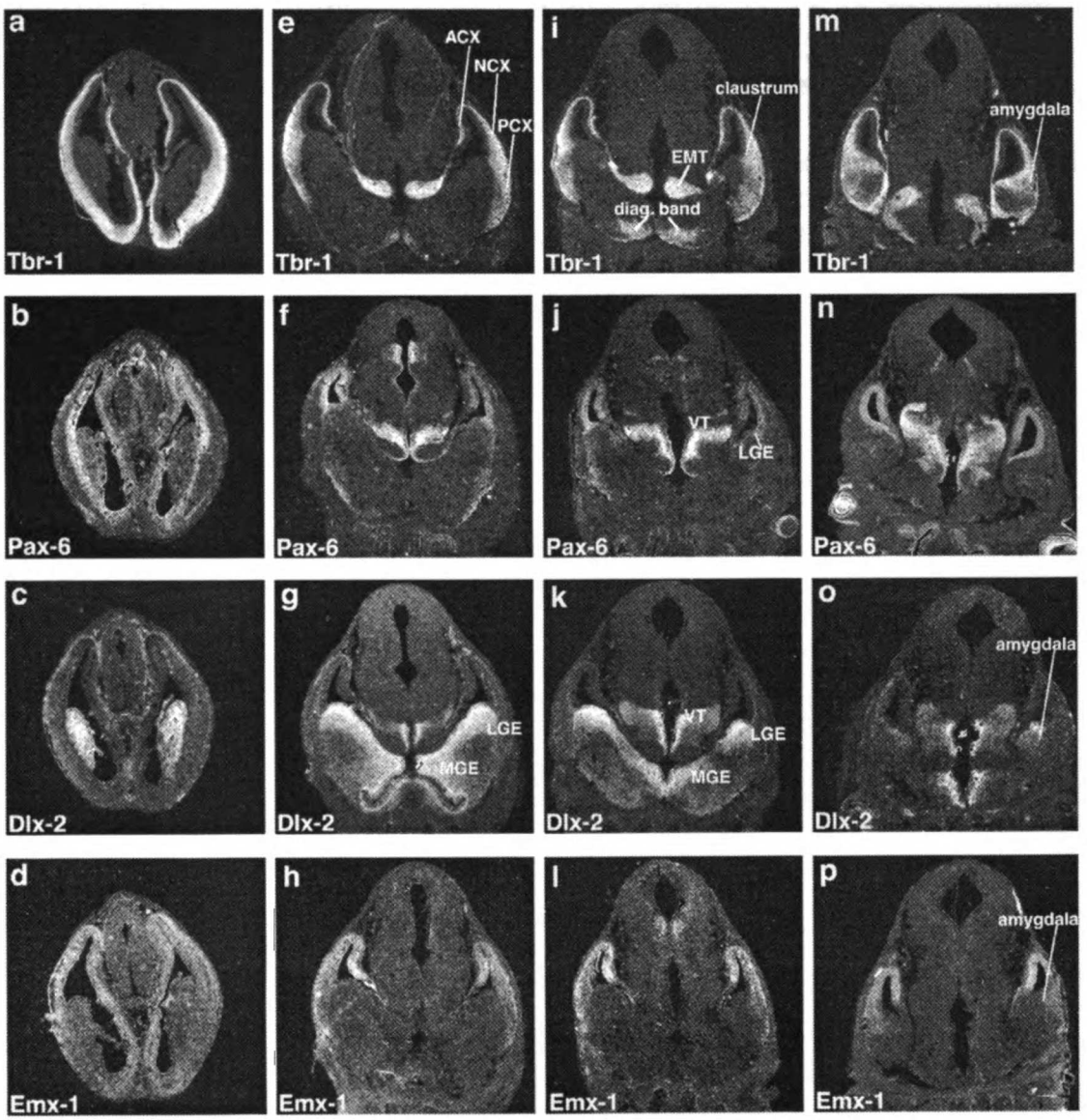

Figure 2.

Comparison of *Nkx-2.1*, *Dlx-2*, *Pax-6*, and *Tbr-1* expression patterns using *in situ* RNA hybridization to chicken E5.0 coronal sections. Sections are ordered rostral (a, b, c, d) to caudal (e, f, g, h).

1st column: a, b, c, d represent section numbers 14, 11, 13, 15, respectively.

2nd column: e, f, g, h represent section numbers 38, 36, 37, 35, respectively.

Sections a and e were analyzed for *Nkx-2.1* expression; sections b and f for *Dlx-2*; sections c and g for *Pax-6*; sections d and h for *Tbr-1* expression.

^{35}S probes were used for all sections. Abbreviations are as defined in the Glossary. All sections were photographed using dark-field microscopy. All sections were from a single chicken embryo (Feather Hill Farms).

Figure 2: Chicken E5.0 coronal sections

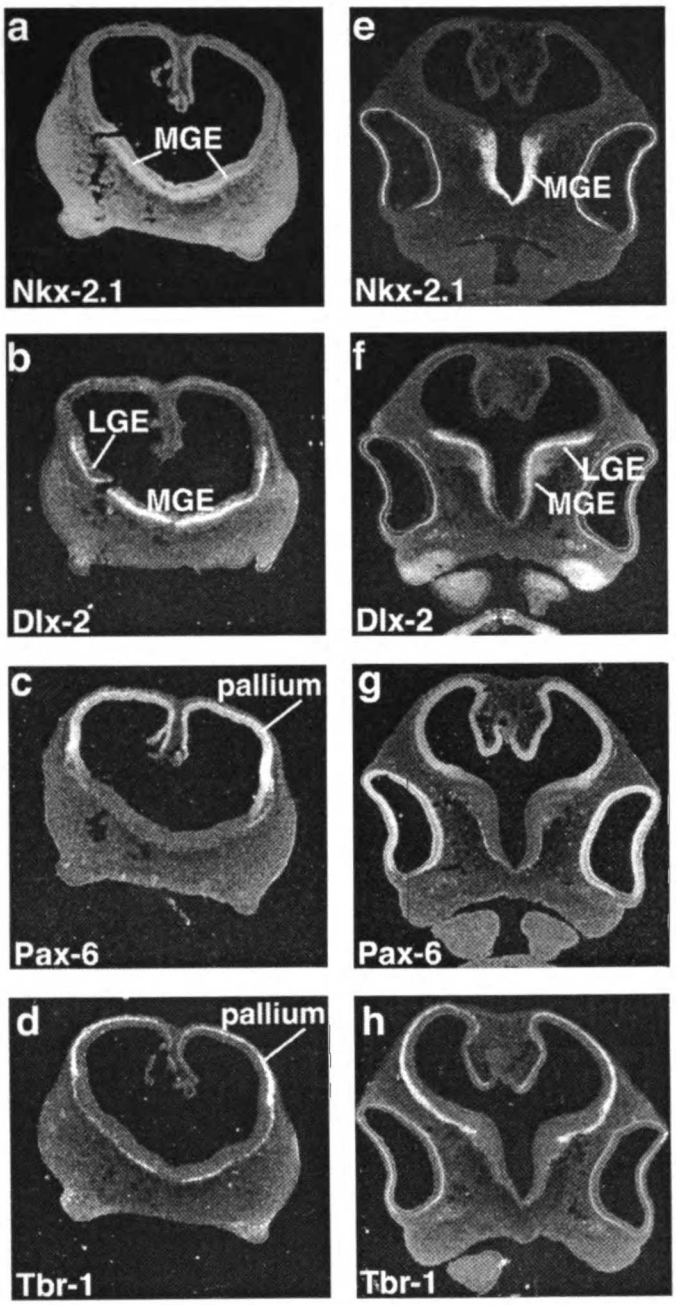

Figure 3.

Comparison of *Nkx-2.1*, *Dlx-2*, *Pax-6*, and *Tbr-1* expression patterns using *in situ* RNA hybridization to chicken E5.0 sagittal sections. Sections are ordered lateral (a) to medial (g).

1st column: a, b, c, d represent section numbers 38, 39, 37, 40, respectively.

2nd column: e, f, g represent section numbers 45, 54, 51, respectively.

Section a was analyzed for *Nkx-2.1* expression; sections b and e for *Dlx-2*; sections c and f for *Pax-6*; sections d and g for *Tbr-1*.

^{35}S probes were used for all sections. Abbreviations are as defined in the Glossary. All sections were photographed using dark-field microscopy. All sections were from a single chicken embryo (Feather Hill Farms).

Figure 3: Chicken E5.0 sagittal sections

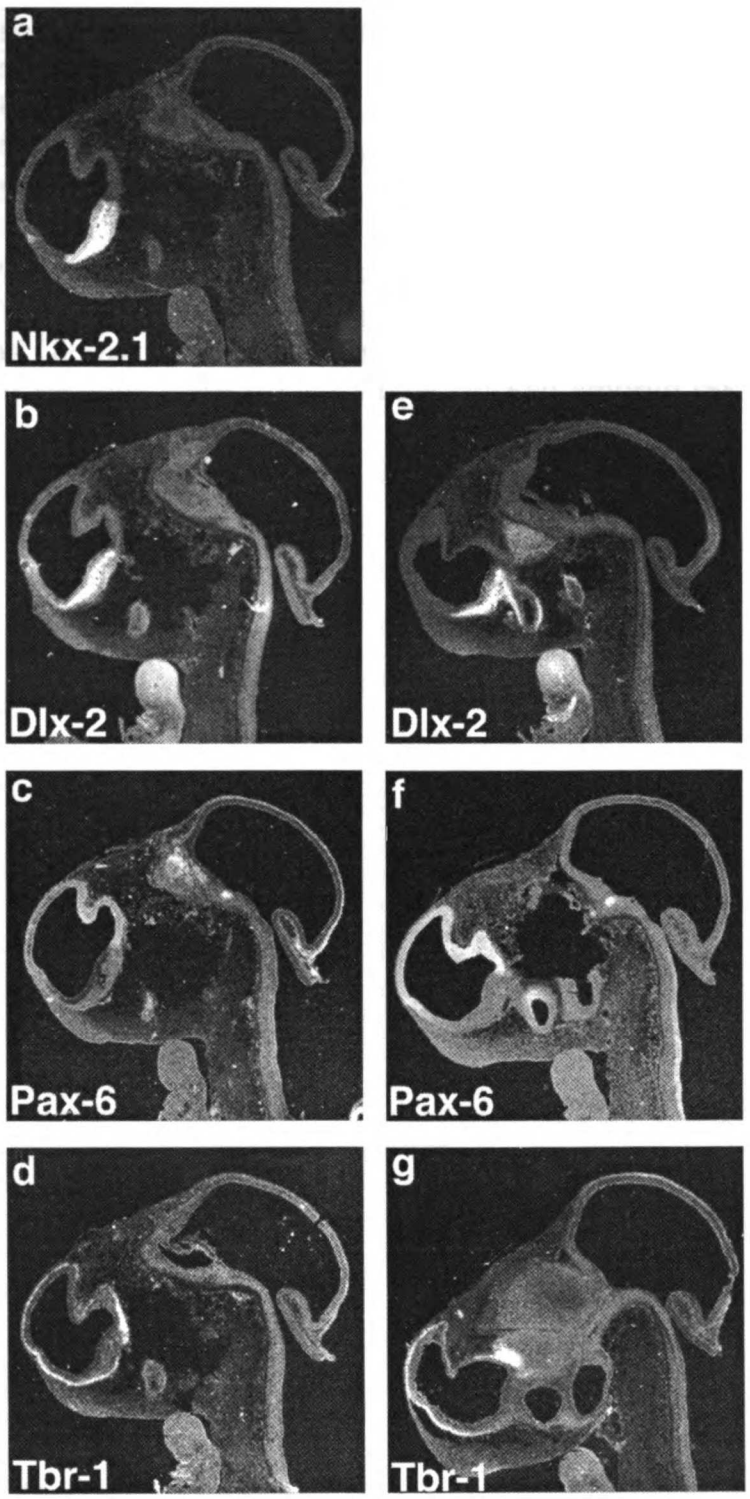

Figure 4.

Comparison of *Nkx-2.1*, *Dlx-2*, *Pax-6*, and *Tbr-1* expression patterns using *in situ* RNA hybridization to chicken E5.0 coronal sections. Sections are ordered rostral (a, b, c, d) to caudal (i, j, k, l).

1st column: a, b, c, d represent section numbers 35, 34, 36, 37, respectively.

2nd column: e, f, g, h represent section numbers 46, 45, 47, 48, respectively.

3rd column: i, j, k, l represent section numbers 77, 76, 78, 79, respectively.

Sections a, e, i were analyzed for *Nkx-2.1* expression; sections b, f, j for *Dlx-2*; sections c, g, k for *Pax-6*; sections d, h, l for *Tbr-1*.

^{35}S probes were used for all sections. Abbreviations are as defined in the Glossary. All sections were photographed using dark-field microscopy. All sections were from a single chicken embryo (SPAFAS).

Figure 4: Chicken E5.0 coronal sections

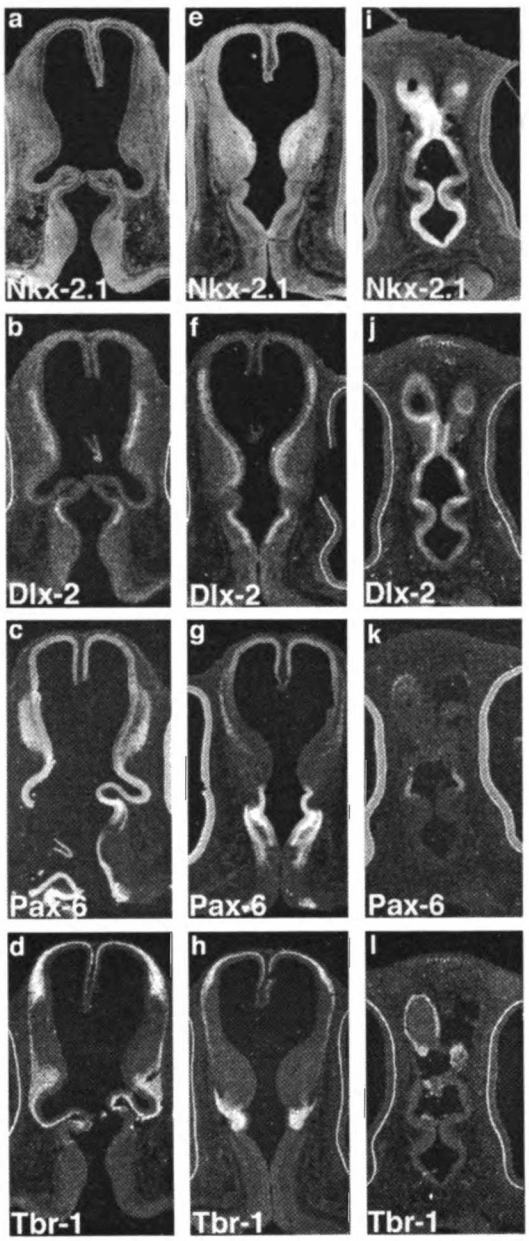

Figure 5.

Comparison of *Dlx-2, Tbr-1, Pax-6,* and *Nkx-2.1* expression patterns using *in situ* RNA hybridization to chicken E8.5 coronal sections. Sections are ordered rostral (a, b, c, d) to caudal (j, k, l, m).

1st column: a, b, c, d represent section numbers 14, 13, 24, 25, respectively.

2nd column: e, f, g, h, i represent section numbers 41, 42, 44, 43, 52, respectively.

3rd column: j, k, l, m represent section numbers 68, 76, 75, 77, respectively.

Sections a, f, l were analyzed for *Dlx-2* expression; sections b, c, e, j, k for *Tbr-1*; sections d, h, i, m for *Pax-6*; section g for *Nkx-2.1.*

^{35}S probes were used for all sections. Abbreviations are as defined in the Glossary. All sections were photographed using dark-field microscopy. All sections were from a single chicken embryo (Feather Hill Farms).

Figure 5: Chicken E8.5 coronal sections

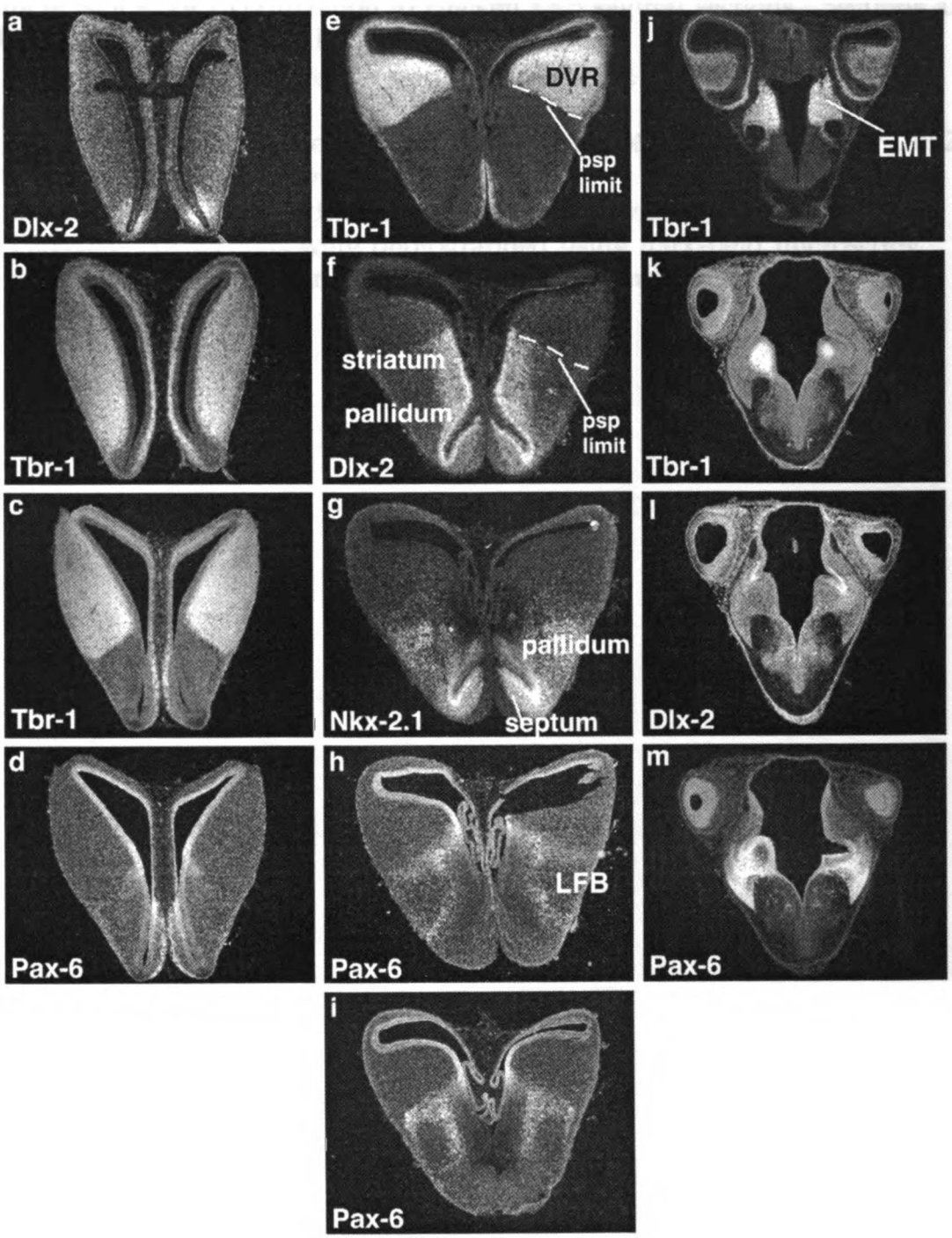

Figure 6.

Comparison of *Tbr-1, Dlx-2, Nkx-2.1,* and *Pax-6* expression patterns using *in situ* RNA hybridization to chicken E8.5 sagittal sections. Sections are ordered lateral (a) to medial (e).

1st column: a, b, c, d, e represent section numbers 28, 41, 42, 44, 43, respectively.

Sections a and b were analyzed for *Tbr-1* expression; section c for *Dlx-2;* section d for *Nkx-2.1;* section e for *Pax-6.*

^{35}S probes were used for all sections. Abbreviations are as defined in the Glossary. All sections were photographed using dark-field microscopy. All sections were from a single chicken embryo (Feather Hill Farms).

Figure 6: Chicken E8.5 sagittal sections

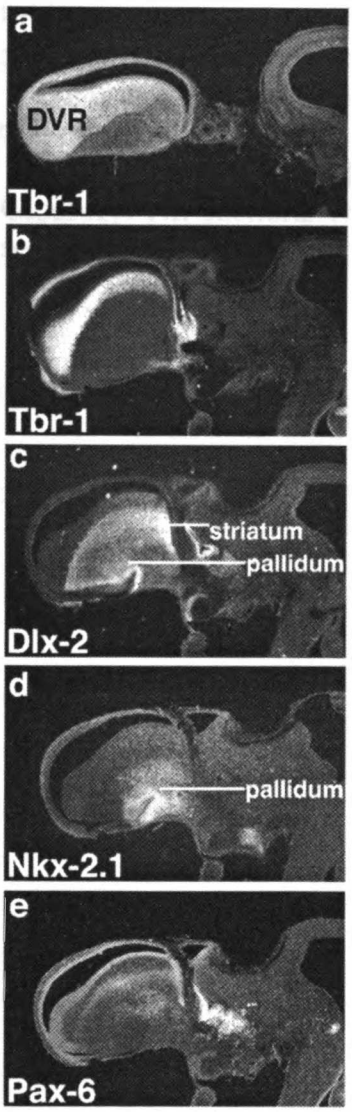

Figure 7.

Comparison of *Tbr-1*, *Pax-6*, and *Dlx-2* expression patterns using *in situ* RNA hybridization to chicken E10.5 coronal sections. Sections are ordered rostral (a) to caudal (c).

1st column: a, b, c represent section numbers 86, 87, 85, respectively.

Section a was analyzed for *Tbr-1* expression; section b for *Pax-6*; section c for *Dlx-2*.

^{35}S probes were used for all sections. Abbreviations are as defined in the Glossary. All sections were photographed using dark-field microscopy. All sections were from a single chicken embryo (Feather Hill Farms).

Figure 7: Chicken E10.5 coronal sections

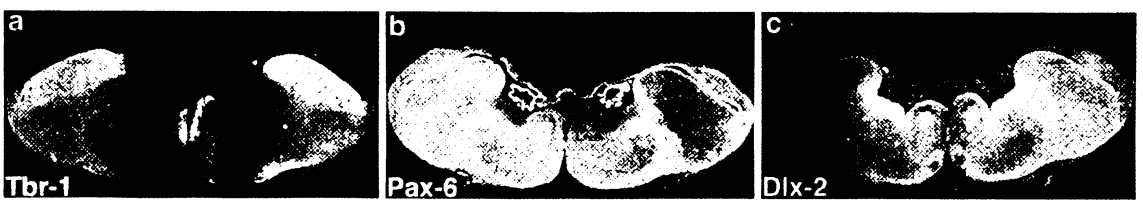

Figure 8.

Comparison of *Tbr-1, Pax-6, Nkx-2.1,* and *Dlx-2* expression patterns using *in situ* RNA hybridization to chicken E10.5 sagittal sections. Sections are ordered lateral (a, b, c) to medial (h, i, j).

1st column: a, b, c represent section numbers 16, 31, 42, respectively.

2nd column: d and e represent section numbers 53 and 54, respectively.

3rd column: f and g represent section numbers 55 and 52, respectively.

4th column: h, i, j represent section numbers 61, 64, 60, respectively.

Sections a, b, c, d, h were analyzed for *Tbr-1* expression; sections e and i for *Pax-6;* section f for *Nkx-2.1;* sections g and j for *Dlx-2* expression.

^{35}S probes were used for all sections. Abbreviations are as defined in the Glossary. All sections were photographed using dark-field microscopy. All sections were from a single chicken embryo (Feather Hill Farms).

Figure 8: Chicken E10.5 sagittal sections

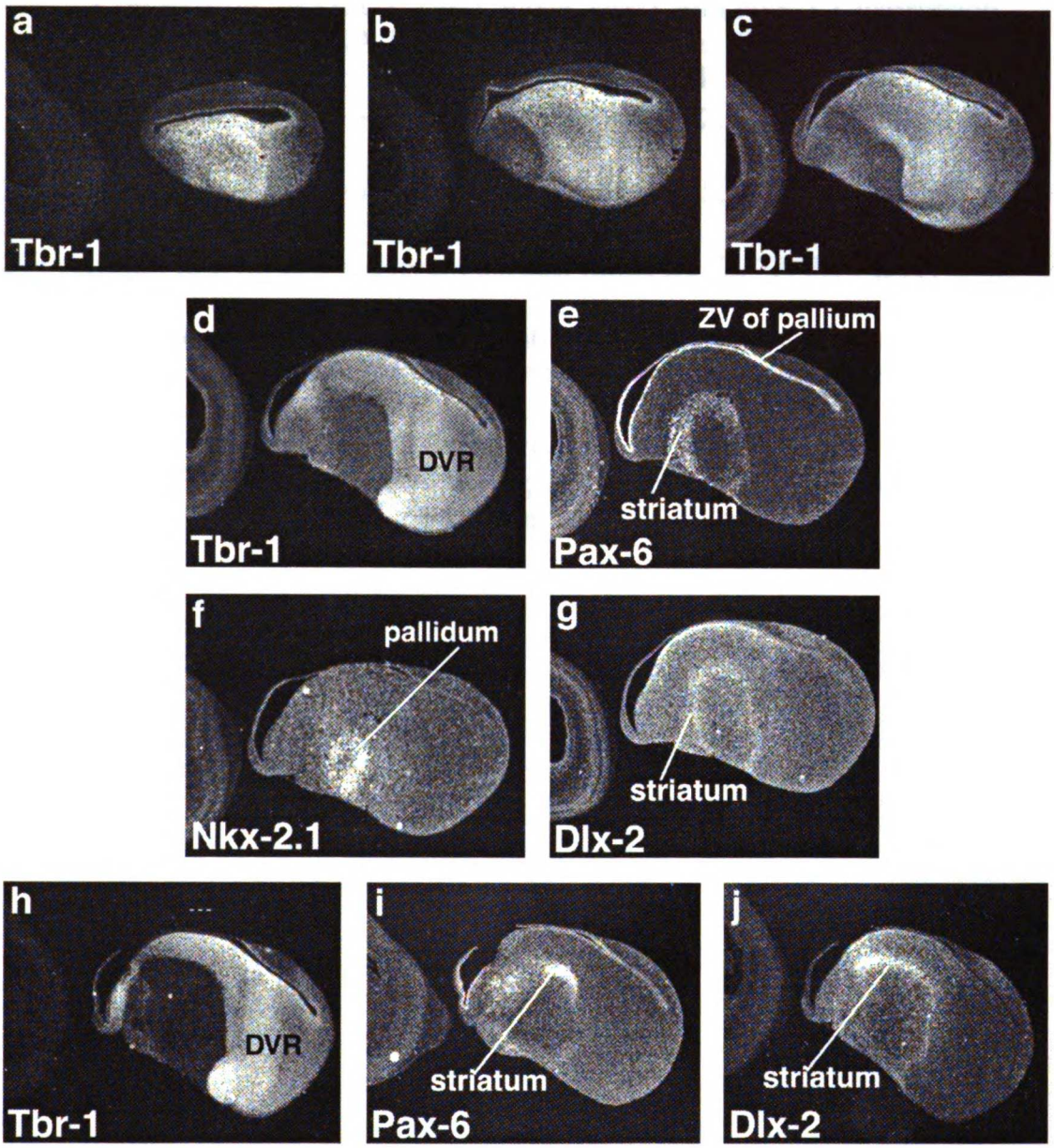

Figure 9.

Comparison of *Emx-1, Tbr-1, Pax-6, Dlx-2,* and *Nkx-2.1* expression patterns using *in situ* RNA hybridization to chicken E10.5 coronal sections. Sections are ordered rostral (a, b, c, d, e) to caudal (k, l, m, n, o).

1st column: a, b, c, d, e represent section numbers 22, 27, 25, 23, 24, respectively.

2nd column: f, g, h, i, j represent section numbers 45, 49, 48, 46, 47, respectively.

3rd column: k, l, m, n, o represent section numbers 73, 77, 76, 74, 75, respectively.

Sections a, f, k were analyzed for *Emx-1* expression; sections b, g, l for *Tbr-1;* sections c, h, m for *Pax-6;* sections d, i, n for *Dlx-2;* sections e, j, o for *Nkx-2.1.*

^{35}S probes were used for all sections. Abbreviations are as defined in the Glossary. All sections were photographed using dark-field microscopy. All sections were from a single chicken embryo (SPAFAS).

Figure 9: Chicken E10.5 coronal sections

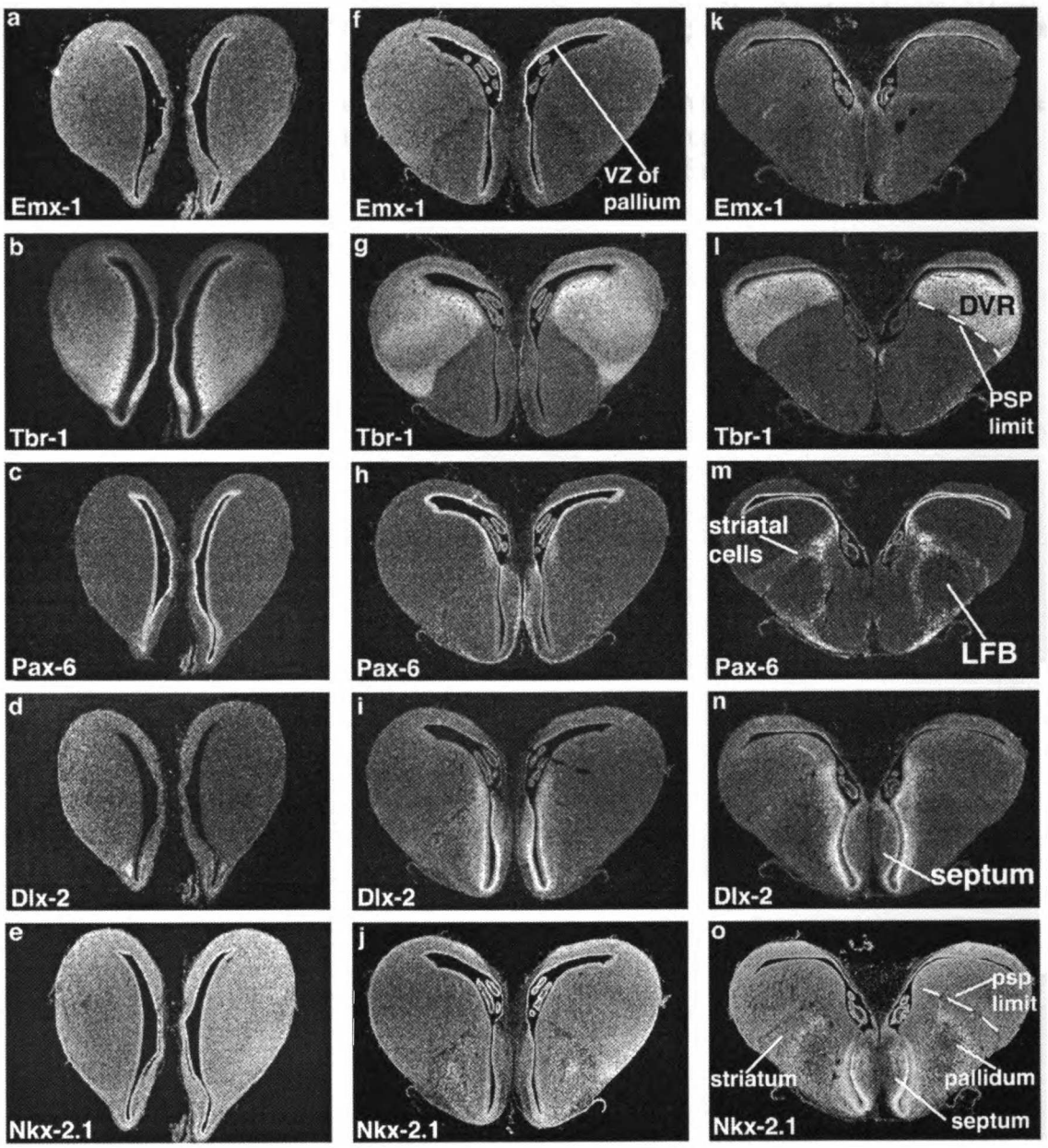

Figure 10.

Comparison of *Tbr-1, Pax-6, Dlx-2,* and *Nkx-2.1* expression patterns using *in situ* RNA hybridization to chicken E14.5 coronal sections.
1st column: a, b, c, d represent section numbers 72, 70, 71, 73, respectively.

Section a was analyzed for *Tbr-1* expression; section b for *Pax-6;* section c for *Dlx-2;* section d for *Nkx-2.1.*

^{35}S probes were used for all sections. Abbreviations are as defined in the Glossary. All sections were photographed using dark-field microscopy. All sections were from a single chicken embryo (Feather Hill Farms).

Figure 10: Chicken E14.5 coronal sections

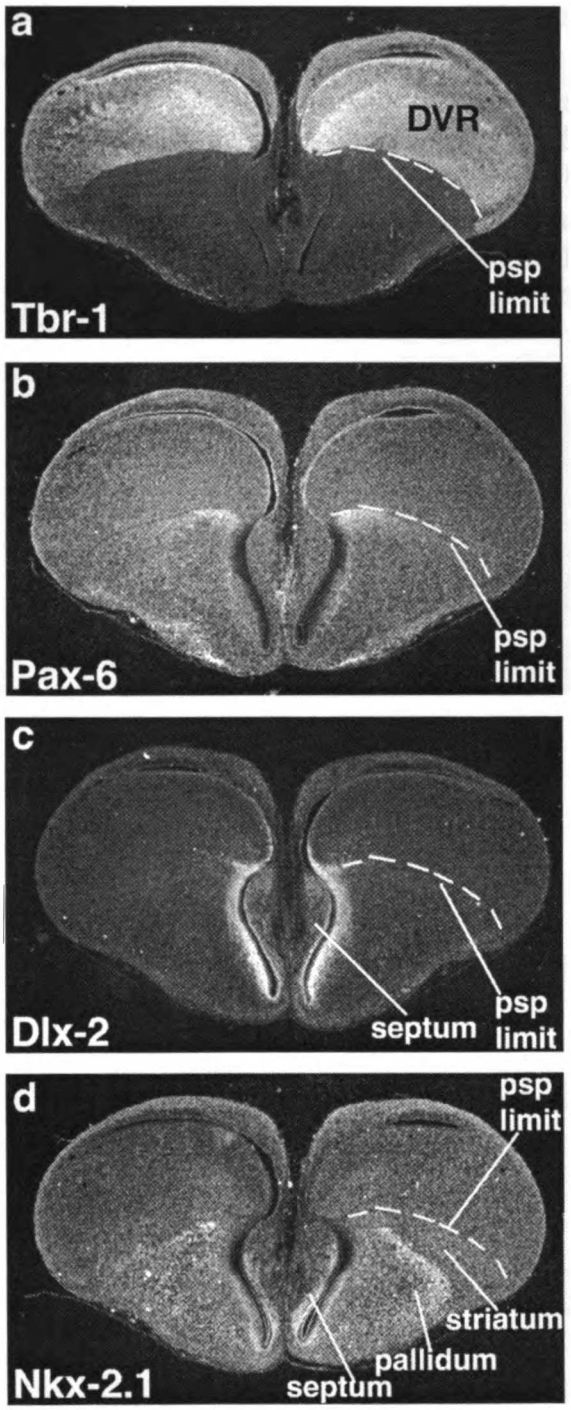

Figure 11.

Comparison of *Tbr-1, Pax-6, Dlx-2,* and *Nkx-2.1* expression patterns using *in situ* RNA hybridization to chicken E14.5 sagittal sections. Sections are ordered lateral (a, b, c, d) to medial (e, f, g, h).

1st column: a, b, c, d represent section numbers 58, 59, 57, 60, respectively.

2nd column: e, f, g, h represent section numbers 72, 70, 71, 92, respectively.

Sections a, e, h were analyzed for *Tbr-1* expression; sections b and f for *Pax-6*; sections c and g for *Dlx-2*; section d for *Nkx-2.1.*

^{35}S probes were used for all sections. Abbreviations are as defined in the Glossary. All sections were photographed using dark-field microscopy. All sections were from a single chicken embryo (Feather Hill Farms).

Figure 11: Chicken E14.5 sagittal sections

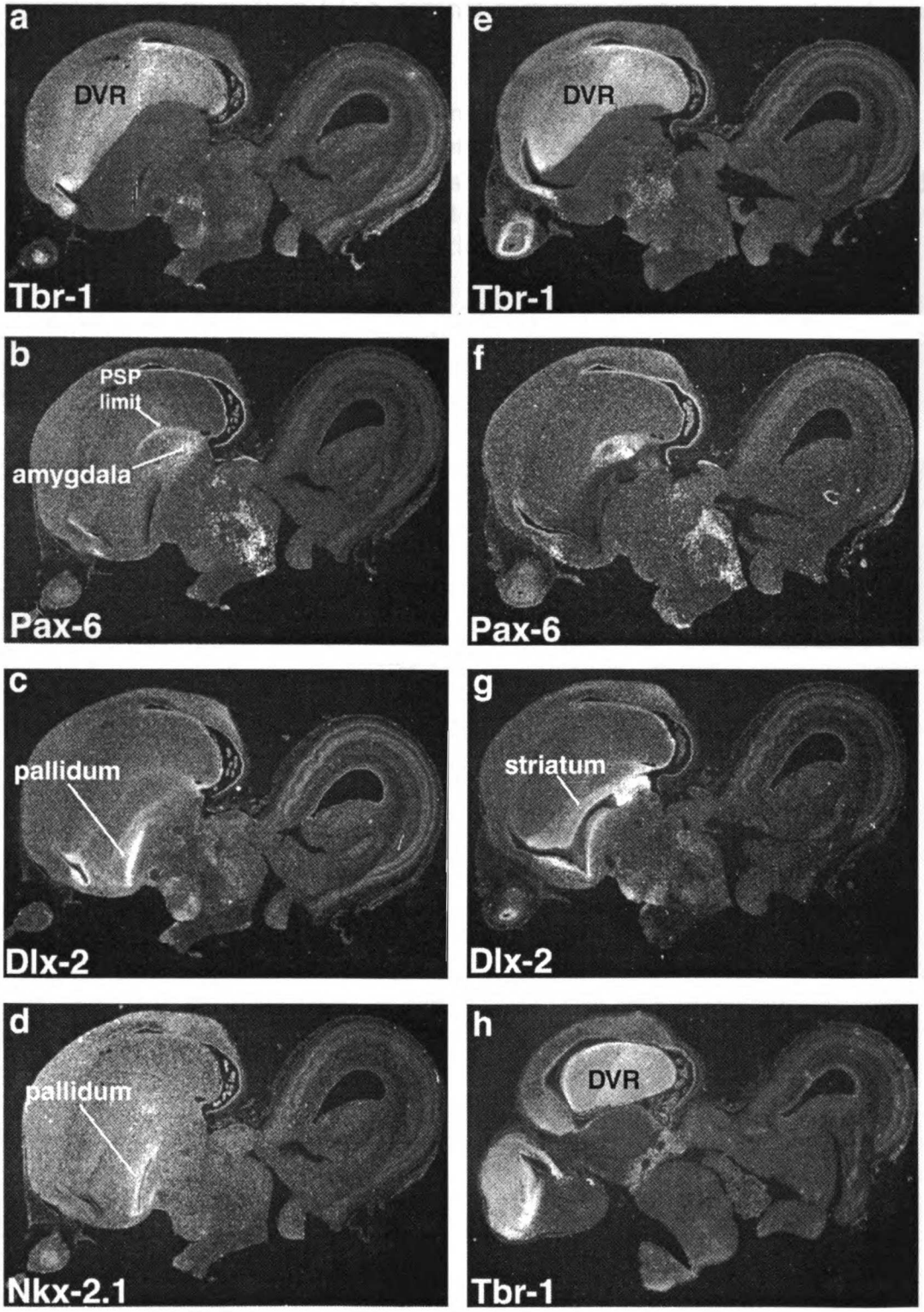

Figure 12.

Comparison of *Tbr-1* expression patterns using *in situ* RNA hybridization to chicken E14.5 coronal sections. Sections are ordered rostral (a, b, c) to caudal (d, e, f).

1st column a, b, c represents section numbers 4, 14, 26 respectively.

2nd column d, e, f represents section numbers 47, 57, 73, respectively.

All sections were analyzed for *Tbr-1* expression.

^{35}S probes were used for all sections. Abbreviations are as defined in the Glossary. All sections were photographed using dark-field microscopy. All sections were from a single chicken embryo (SPAFAS).

Figure 12: Chicken E14.5 coronal sections

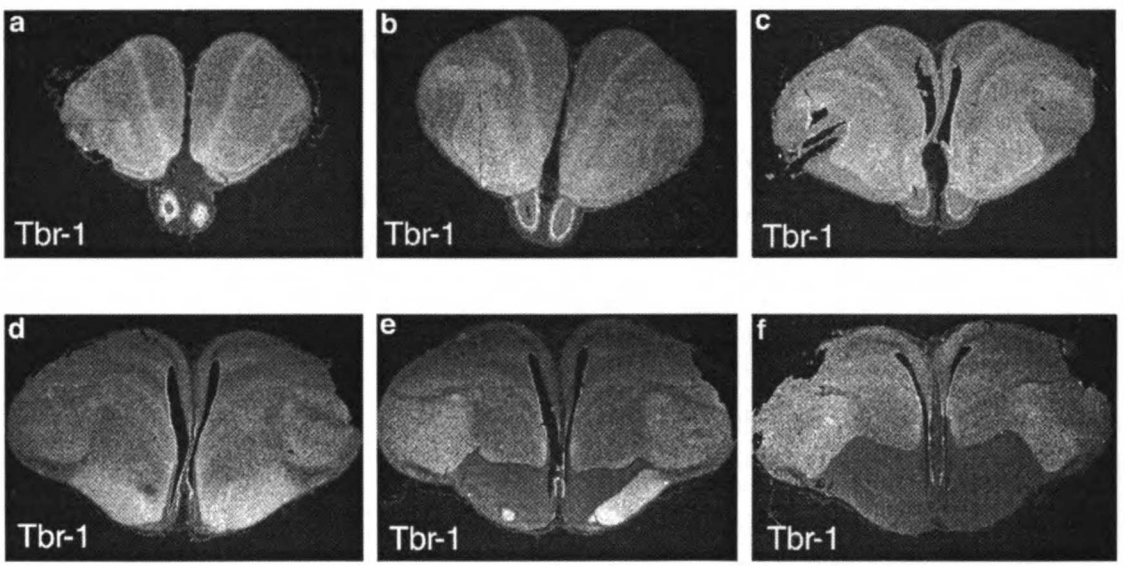

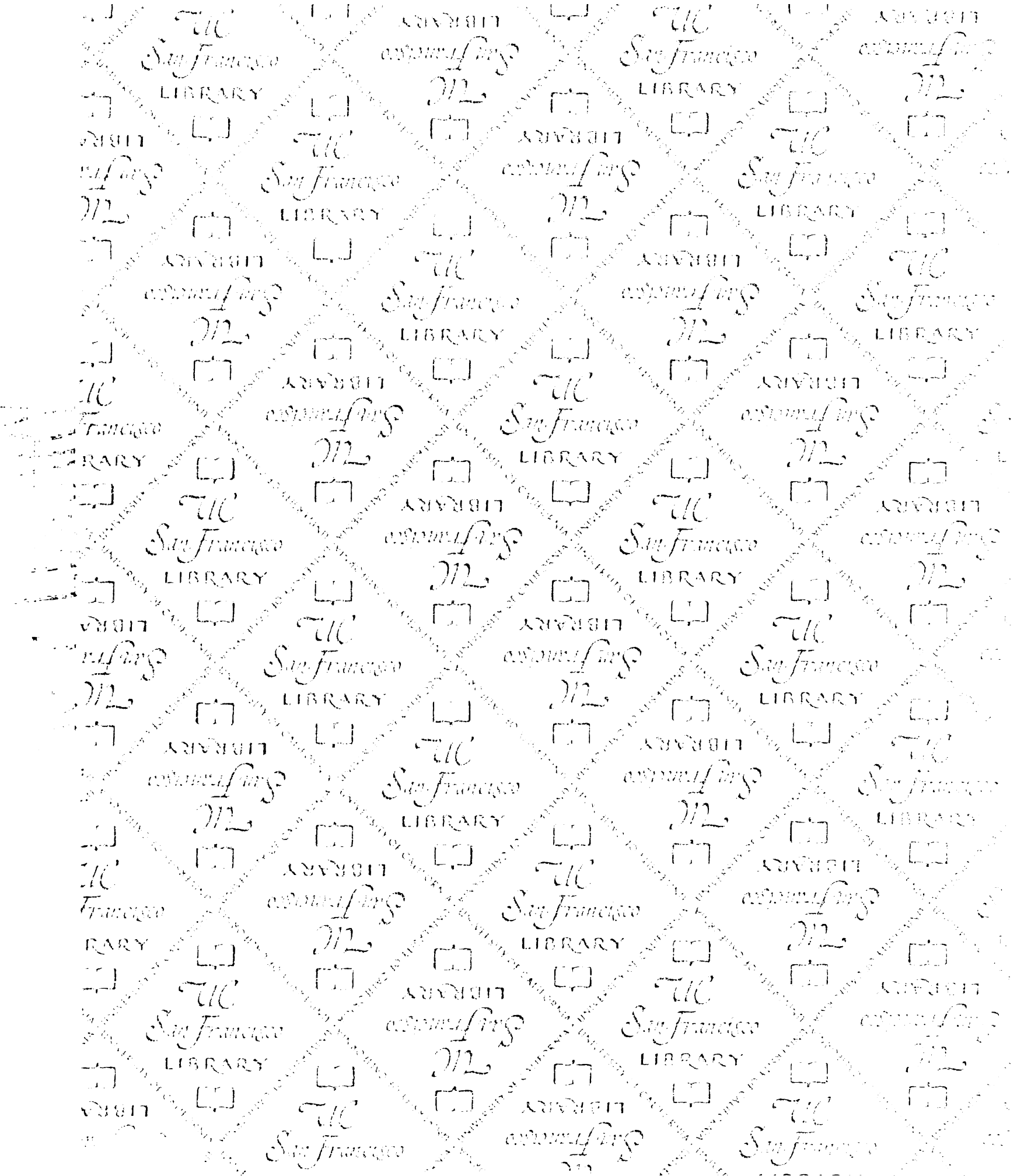
The San Francisco LIBRARY